NATIONAL ADVISORY COMMITTEE FOR AERONAUTICS

TECHNICAL NOTE 2456

3

ANALYTICAL METHOD FOR DETERMINING PERFORMANCE OF TURBOJET-ENGINE TAIL-PIPE HEAT EXCHANGERS

By Michael Behun and Harrison C. Chandler, Jr.

Lewis Flight Propulsion Laboratory
Cleveland, Ohio

Washington

September 1951

NATIONAL ADVISORY COMMITTEE FOR AERONAUTICS

TECHNICAL NOTE 2456

ANALYTICAL METHOD FOR DETERMINING PERFORMANCE OF TURBOJET-ENGINE TAIL-PIPE HEAT EXCHANGERS

By Michael Behun and Harrison C. Chandler, Jr.

SUMMARY

The performance of parallel-flow-type tail-pipe heat exchangers is analytically investigated. An equation is developed relating the output of unfinned heat exchangers to the inlet- and outlet-air temperatures, engine-temperature ratio, corrected engine gas flow per unit of tail-pipe area, and heat-exchanger dimensions.

The calculated performance of heat exchangers, based on assumed characteristics of a hypothetical engine (rated compressor pressure ratio, 4 and rated engine-temperature ratio, 3.4), are presented in the form of generalized working charts for heat-exchanger outlet air temperatures of 700° to 1100° R and flight conditions representative of climb and cruise operation. The use of these working charts to predict the performance of heat exchangers installed on engines having higher compressor-pressure ratios will give results that are optimistic. The method of calculating heat-exchanger performance as set forth in this analysis, however, is still applicable.

The use of the generalized working charts to predict the performance of unfinned heat exchangers is explained and the consideration of such factors as pressure drop through the air side of the heat exchanger and effect on engine performance is discussed. It is shown that, in general, the extraction of heat from the tail-pipe gas by means of a ram-operated unfinned tail-pipe heat exchanger has only a slight effect on engine performance. The addition of longitudinal fins to the air side of the heat exchanger in order to increase the heat output per unit of heat exchanger length is also considered.

A comparison of the performances of parallel-flow-type finned and unfinned tail-pipe heat exchangers on the basis of equal pressure drop through the air side at high heat outputs indicates that the unfinned heat exchanger because of its lighter weight and simpler construction is probably preferable to the longitudinally finned heat exchanger.

INTRODUCTION

One of the principal aspects of the problem of protecting turbojet-powered aircraft against ice accretion is the selection and design of a satisfactory heat source for the thermal anti-icing system. The problem is particularly pertinent to aircraft designed for all-weather operation.

The NACA Lewis laboratory has undertaken a program of analytical study to evaluate the effect on turbojet-engine performance of extracting energy from several points in the engine cycle. The program included an investigation of the effects of air bleed from the compressor outlet, hot gas bleed from the turbine inlet, hot gas bleed from the turbine outlet, and shaft power extraction (references 1 to 4).

Energy can also be extracted from the engine cycle by means of a tail-pipe heat exchanger. Inasmuch as the tail-pipe heat exchanger consists of a shroud surrounding the tail pipe of a turbojet engine, the heat exchanger has no resistance to the flow of gases through the tail pipe. Because of this fact and the large mass of hot gas that flows through the tail pipe, the tail-pipe heat exchanger offers interesting possibilities as a source of heat for thermal anti-icing systems of turbojet-powered aircraft.

Thus, an analytical investigation has been carried out to determine and to evaluate the performance of parallel-flow-type tail-pipe heat exchangers installed on a nonafterburning turbojet engine.

In the analytical investigation of the performance of tail-pipe heat exchangers, three main phases are considered: (1) the method of analysis and the development of generalized working charts expressing the performance of unfinned heat exchangers; (2) calculation of engine performance with heat exchanger in operation; and (3) comparison of the performance of unfinned and longitudinally finned heat exchangers.

The analysis, which is based on conventional heat-transfer equations, relates the heat output to the heat-exchanger inlet and outlet air temperatures, engine temperature ratio, corrected engine gas flow per unit of tail-pipe area and heat-exchanger dimensions. Generalized working charts giving the performance of unfinned tail-pipe heat exchangers installed on a hypothetical engine are presented for flight conditions representative of climb and cruise operation for a range of altitudes and heat-exchanger outlet air temperatures.

The effect of a tail-pipe heat exchanger on the engine cycle performance is given for a range of corrected engine speeds and tail-pipe total-temperature ratios. The effect of the inlet momentum drag (of a ram-operated heat exchanger) and the pumping loss resulting from the extraction of power from the engine to force the air through the air side of the heat exchanger are also considered.

The heat output of unfinned and longitudinally finned heat exchangers is compared on the basis of: (1) equal heat-exchanger length, passage height, and outlet-air temperature; and (2) equal heat-exchanger length, outlet-air temperature, and pressure drop through the air side of the heat exchanger.

SYMBOLS

The following symbols are used in this report:

A	flow area, (sq ft)
C_1, C_2	constants
c_p	specific heat at constant pressure, (Btu/(lb)($^\circ$F))
D	diameter, (ft)
D_h	hydraulic diameter, (ft) $\frac{4 \times \text{cross-sectional area}}{\text{wetted perimeter}}$
F_n	net thrust, (lb)
h	heat-transfer coefficient, (Btu/(hr)(sq ft)($^\circ$F))
k	thermal conductivity, (Btu/(hr)(ft)($^\circ$F))
l	length of heat exchanger, (ft)
N	engine speed, (rpm)
n	number of fins
P	total pressure, (lb/sq ft abs.)
q	heat flow, (Btu/hr)
S	surface area for heat transfer, (sq ft)
s	fin thickness, (ft)
T	mean temperature of fluid, ($^\circ$R)
U	effective over-all heat-transfer coefficient, (Btu/(hr)(sq ft)($^\circ$F))
W	weight flow, (lb/hr)

y	height of passage, (ft)
δ	ratio of total pressure to NACA standard sea-level pressure, P/2116
θ	ratio of total temperature to NACA standard sea-level temperature, T/519

Subscripts:

a	air
f	finned heat exchanger
g	gas
R	rated
u	unfinned heat exchanger
w	wall
0	ambient conditions
1	compressor inlet
2	turbine inlet
3	turbine outlet
4	tail-pipe outlet
5	exhaust-nozzle outlet
6	heat-exchanger air inlet
7	heat-exchanger air outlet

CONFIGURATIONS

The two types of parallel-flow tail-pipe heat exchanger investigated are shown in figure 1. An unfinned heat exchanger consisting of an annular shroud surrounding the tail pipe of a turbojet engine is shown in figure 1(a). Air enters the heat exchanger at station 6, is heated as it flows along the annular passage, and is discharged at station 7 into the duct connecting the heat exchanger with the

anti-icing system. Figure 1(b) shows a longitudinally finned heat exchanger in which the fin height is equal to the passage height (one-half the difference between the outer and inner diameter) and the fin length is equal to the heat-exchanger length.

BASIC ASSUMPTIONS

The following basic assumptions were made in the development of the equation expressing the performance of a parallel-flow, annular-type tail-pipe heat exchanger:

(1) Steady-state conditions

(2) Heat-exchanger flow passages of constant cross-sectional area

(3) Uniform transverse temperature distribution in annulus and tail pipe

(4) Constant exhaust-gas temperature from inlet to outlet

(5) Fully developed turbulent flow

(6) Negligible radiant heat transfer

(7) Negligible temperature drop across inside wall and no longitudinal conduction

(8) No heat flow through outside wall

ANALYSIS

Under steady-state conditions, the rate of heat transfer from the exhaust gas through a thin separating wall to the air flowing over the outer surface of the tail pipe is given by

$$q = US(T_g - T_a) \tag{1}$$

where U is the over-all heat-transfer coefficient, S the heat-transfer area, and $(T_g - T_a)$ the effective mean temperature difference. The factor US is related to the individual heat-transfer coefficients as

$$\frac{1}{US} = \frac{1}{S_a h_a} + \frac{1}{S_g h_g} \tag{2}$$

The individual heat-transfer coefficient depends on the fluid and the flow conditions. Reference 5 gives the following relation for fully developed turbulent flow of air or exhaust gas in long ducts:

$$h = 5.4\times10^{-4}\frac{T^{0.3}\left(\frac{W}{A}\right)^{0.8}}{D_h^{0.2}} \tag{3}$$

where T is the mean temperature of the fluid ($^{\circ}R$), W/A the weight flow per unit area (lb/(hr)(sq ft)), and D_h the hydraulic diameter (ft). Substitution of equation (3) (with proper subscripts) into equation (2) gives

$$\frac{1}{US} = \frac{1}{5.4\times10^{-4}}\left[\frac{D_{h,a}^{0.2}}{S_a T_a^{0.3}\left(\frac{W_a}{A_6}\right)^{0.8}} + \frac{D_{h,g}^{0.2}}{S_g T_g^{0.3}\left(\frac{W_g}{A_4}\right)^{0.8}}\right] \tag{4}$$

Inasmuch as the air flow through the heat exchanger, for the range of outlet-air temperatures of interest, will be quite small in proportion to the engine gas flow, the decrease in gas temperature in the tail pipe will also be small. Consequently, the simplifying assumption that the mean gas temperature in the tail pipe T_g is equal to the turbine-outlet gas temperature T_3 may be made. With this change made in equation (4) and with the engine gas flow per unit of tail-pipe area corrected to NACA standard sea-level conditions, the equation becomes

$$\frac{5.4\times10^{-4}}{US} = \frac{D_{h,a}^{0.2}}{S_a T_a^{0.3}\left(\frac{W_a}{A_6}\right)^{0.8}} + \frac{D_{h,g}^{0.2}\,T_1^{0.1}}{S_g (T_3/T_1)^{0.3}\left(\frac{W_g\sqrt{\theta_1}}{A_4\delta_1}\right)^{0.8}\delta_1^{0.8}(519)^{0.4}} \tag{5}$$

Multiplying the left side of equation (5) by $\frac{W_a c_{p,a}}{W_a c_{p,a}}$ and replacing T_a by its equivalent, $\frac{T_7+T_1}{2}$, give

$$\left(\frac{W_a c_{p,a}}{US}\right)\left(\frac{5.4\times10^{-4}}{W_a c_{p,a}}\right) = \frac{1.231\,D_{h,a}^{0.2}}{S_a T_1^{0.3}\left(\frac{T_7}{T_1}+1\right)^{0.3}\left(\frac{W_a}{A_6}\right)^{0.8}} + \frac{D_{h,g}^{0.2}\,T_1^{0.1}}{12.2\,S_g\left(\frac{T_3}{T_1}\right)^{0.3}\left(\frac{W_g\sqrt{\theta_1}}{A_4\delta_1}\right)^{0.8}\delta_1^{0.8}} \tag{6}$$

The heat removed from the tail-pipe gas is given by

$$q = W_a c_{p,a} T_1 \left(\frac{T_7}{T_1} - 1\right) \tag{7}$$

Solving equation (7) for W_a and substituting into equation (6) give

$$5.4\times10^{-4}\left(\frac{W_a c_{p,a}}{US}\right)\frac{T_1\left(\frac{T_7}{T_1} - 1\right)}{q} = \frac{1.231\, D_{h,a}^{0.2} A_6^{0.8} (c_{p,a})^{0.8} T_1^{0.5}\left(\frac{T_7}{T_1} - 1\right)^{0.8}}{S_a q^{0.8} (T_7/T_1 + 1)^{0.3}} + \frac{D_{h,g}^{0.2}\, T_1^{0.1}}{12.2\, S_g\left(\frac{T_3}{T_1}\right)^{0.3}\left(\frac{W_g\sqrt{\theta_1}}{A_4\delta_1}\right)^{0.8}\delta_1^{0.8}} \tag{8}$$

Assuming $c_{p,a} = 0.24$ and rearringing terms give

$$\frac{1.83\left(\frac{W_a c_{p,a}}{US}\right)\theta_1^{0.4}(T_7/T_1 - 1)}{\left(\frac{q}{S_g\sqrt{\theta_1}}\right)} = \frac{58.5\, S_g^{0.2} D_{h,a}^{0.2} A_6^{0.8}\left(\frac{T_7}{T_1} - 1\right)^{0.8}}{S_a\left(\frac{q}{S_g\sqrt{\theta_1}}\right)^{0.8}\left(\frac{T_7}{T_1} + 1\right)^{0.3}} + \frac{D_{h,g}^{0.2}}{\left(\frac{T_3}{T_1}\right)^{0.3}\left(\frac{W_g\sqrt{\theta_1}}{A_4\delta_1}\right)^{0.8}\delta_1^{0.8}} \tag{9}$$

Transposing and gathering terms,

$$\frac{D_{h,a}^{0.2} A_6^{0.8} S_g^{0.2}}{S_a} = \frac{\left(\frac{q}{S_g\sqrt{\theta_1}}\right)^{0.8}\left(\frac{T_7}{T_1} + 1\right)^{0.3}}{58.5(T_7/T_1 - 1)^{0.8}}\left[\frac{1.83\left(\frac{W_a c_{p,a}}{US}\right)\left(\frac{T_7}{T_1} - 1\right)\theta_1^{0.4}}{\left(\frac{q}{S_g\sqrt{\theta_1}}\right)} - \frac{D_{h,g}^{0.2}}{\left(\frac{T_3}{T_1}\right)^{0.3}\left(\frac{W_g\sqrt{\theta_1}}{A_4\delta_1}\right)^{0.8}\delta_1^{0.8}}\right] \tag{10}$$

Inasmuch as the hydraulic diameter of a circular duct is equal to the geometric diameter and the heat-transfer area on the gas side S_g may be expressed as $\pi D_4 l$, equation (10) becomes

$$\frac{D_{h,a}^{0.2} A_6^{0.8} D_4^{0.2} l^{0.2}}{S_a} = \frac{\left(\frac{q}{D_4 l \sqrt{\theta_1}}\right)^{0.8} \left(\frac{T_7}{T_1} + 1\right)^{0.3}}{183.7 \left(\frac{T_7}{T_1} - 1\right)^{0.8}} \left[\frac{5.746 \left(\frac{W_a c_{p,a}}{US}\right) \left(\frac{T_7}{T_1} - 1\right) \theta_1^{0.4}}{\left(\frac{q}{D_4 l \sqrt{\theta_1}}\right)} - \frac{D_4^{0.2}}{\left(\frac{T_3}{T_1}\right)^{0.3} \left(\frac{W_g \sqrt{\theta_1}}{A_4 \delta_1}\right)^{0.8} \delta_1^{0.8}} \right] \tag{11}$$

The parameter $\frac{W_a c_{p,a}}{US}$ in equation (11) is related to the fluid temperatures as follows (see the appendix for derivation):

$$\frac{\frac{T_7}{T_1} - 1}{\frac{T_3}{T_1} - 1} = 1 - \left(\frac{\frac{T_3}{T_1} - \frac{T_6}{T_1}}{\frac{T_3}{T_1} - 1} \right) e^{-\left(\frac{US}{W_a c_{p,a}}\right)} \tag{12}$$

For a ram-operated heat exchanger, T_6 is equal to T_1 and equation (12) becomes

$$\frac{\frac{T_7}{T_1} - 1}{\frac{T_3}{T_1} - 1} = 1 - e^{-\left(\frac{US}{W_a c_{p,a}}\right)} \tag{13}$$

Figure 2 is a plot of equation (13).

For an unfinned annular passage, the hydraulic diameter D_h is equal to twice the passage height and the air-flow area A_6 may be closely approximated by $\pi D_4 y$. The heat-transfer area on the air side of the heat exchanger is equal to the heat-transfer area on the gas side $\pi D_4 l$. For an unfinned tail-pipe heat exchanger, equation (11) reduces to

$$\frac{y}{l^{0.8}} = \frac{\left(\frac{q}{D_4 l\sqrt{\theta_1}}\right)^{0.8}\left(\frac{T_7}{T_1}+1\right)^{0.3}}{167.8\left(\frac{T_7}{T_1}-1\right)^{0.8}}\left[\frac{5.746\left(\frac{W_a c_{p,a}}{US}\right)\left(\frac{T_7}{T_1}-1\right)\theta_1^{0.4}}{\left(\frac{q}{D_4 l\sqrt{\theta_1}}\right)} - \frac{D_4^{0.2}}{\left(\frac{T_3}{T_1}\right)^{0.3}\left(\frac{W_g\sqrt{\theta_1}}{A_4\delta_1}\right)^{0.8}\delta_1^{0.8}}\right] \tag{14}$$

Equation (14) relates the heat output to the fluid temperatures, corrected engine gas flow per unit of tail-pipe area, and heat exchanger dimensions.

Heat-transfer theory indicates that the addition of fins to the air side of the tail-pipe heat exchanger should appreciably increase the heat output per unit length of the heat exchanger. Therefore, the addition of longitudinal fins to the air side of the heat exchanger can be expected to increase the heat output of a heat exchanger of given length or decrease the length of a heat exchanger required to deliver a given heat output.

Although equation (11) is general, it does not lend itself readily to the calculation of the performance of finned heat exchangers. Consequently the finned heat-exchanger performance presented herein was calculated using the following expression derived from reference 5:

$$l_f = \frac{q}{\left[n\sqrt{2skh_f}\tanh y\sqrt{\frac{2h_f}{sk}} + (\pi D - ns)h_a\right](T_w - T_a)} \tag{15}$$

CALCULATIONS AND PRESENTATION OF GENERALIZED WORKING CHARTS

Analysis of the icing problem indicates that for a typical hot-gas type thermal anti-icing system installed on turbojet-powered transport aircraft the maximum heat requirements occur at a flight Mach number of 0.5 at an altitude of 15,000 feet. The flight conditions therefore considered to be of greatest interest were a Mach number of 0.5 at altitudes from 5000 to 35,000 feet and a Mach number of 0.7 at altitudes from 25,000 to 35,000 feet; these flight conditions are considered to be representative of climb and cruise operation, respectively, of most types of turbojet-powered aircraft.

The performance of unfinned tail-pipe heat exchangers installed on a hypothetical nonafterburning turbojet engine was calculated using equation (14). The heat-exchanger inlet air temperature was assumed to be equal to the temperature of the ram air at each flight condition investigated.

The hypothetical engine assumed in these calculations was considered to be representative of turbojet engines having a nominal compressor-pressure ratio of 4.0, a rated engine-temperature ratio of 3.4, and a rated corrected gas flow per unit of tail-pipe area of 40 pounds per second per square foot. The relation between engine gas flow and corrected engine speed and the basic engine pumping characteristics (engine total-pressure ratio P_3/P_1 against total-temperature ratio T_3/T_1) for corrected engine speeds of 0.9, 1.0, and 1.1 times the rated value are presented in figure 3. For generality, all quantities are presented as fractions of their values when the engine is operating at rated engine speed and standard sea-level engine-inlet conditions. For the climb condition, the engine was assumed to operate at rated engine speed and a turbine-inlet temperature of 2000° R. Operation during cruise was assumed to be at 95 percent of rated engine speed and a turbine-inlet temperature ratio T_2/T_1 of 95 percent of its rated value. The range of other variables used in these calculations were:

Tail-pipe diameter, ft	1.5 to 2.17
Tail-pipe length, ft	4 to 10
Heat-exchanger outlet air temperature, °R	700 to 1100

The results of the performance calculations of unfinned tail-pipe heat exchangers for the climb condition (Mach number of 0.5 at altitudes from 5000 to 35,000 ft) are presented in the form of generalized working charts in figure 4. The performance for heat-exchanger outlet-air temperatures of 800° to 1100° R is expressed in terms of a heat-output parameter $q/Dl\sqrt{\theta_1}$, an air-flow parameter W_a/Dl $\left(\text{where } \frac{W_a}{Dl} = \frac{\frac{q}{Dl}}{c_{p,a}(T_7-T_1)}\right)$, and a ratio of heat-exchanger length to passage height $l^{0.8}/y$. Similar generalized working charts showing the performance of heat exchangers at the cruising flight condition (Mach number of 0.7 at altitudes from 25,000 to 35,000 ft) are presented in figure 5 for outlet-air temperatures of 700° to 1000° R.

Limitations of Working Charts

As indicated previously, the calculated performance of heat exchangers as given in the generalized working charts was based on assumed component characteristics of a hypothetical engine. The

accuracy in predicting the performance of heat exchangers installed on an engine of different design would depend on the similarity between the characteristics of that engine and the engine characteristics used in computing the generalized working charts.

The engine characteristics affecting the performance of an unfinned tail-pipe heat exchanger, as given by equations (13) and (14), are engine temperature ratio and corrected engine gas flow. The present trend in engine design is toward higher compressor pressure ratios and higher turbine-inlet temperatures. However, because of metallurgical limitations, the increase in turbine-inlet temperature has not been as great as the increase in pressure ratio. Consequently, the increase in pressure ratio has been accompanied by a decrease in engine temperature ratio.

An indication of the magnitude of the effect of increased compressor pressure ratio (and consequently reduced engine temperature ratio) on heat-exchanger performance as obtained by use of the working charts is given by the following example. Assume a heat exchanger having a diameter of 2.17 feet and a length of 6 feet to be installed on an engine having a nominal compressor-pressure ratio of 10; the corresponding engine temperature ratio is 10 percent lower than that assumed for the hypothetical engine. In addition, assume the required output of the heat exchanger, at an outlet-air temperature of 800° R, to be 750,000 Btu per hour at a flight Mach number of 0.5 and an altitude of 15,000 feet.

If figure 4 were employed to design this heat exchanger, the result would be a configuration operating at an outlet-air temperature T_7 of 750° R rather than 800° R and delivering a heat output 84 percent of the design value, because of the lower engine tail-pipe gas temperature. In order to attain the design heat output of 750,000 Btu per hour at the flight condition specified, the passage height on the air side of the heat exchanger would have to be reduced 28 percent below the value obtained from figure 4.

In the case of a turbojet engine having a corrected engine gas flow per unit of tail-pipe area 20 percent greater than that of the assumed hypothetical engine, use of figure 4 for the design problem just described would produce an opposite effect. The heat exchanger would operate at an outlet-air temperature of 816° R rather than 800° R and deliver a heat output 5 percent greater than the design value of 750,000 Btu per hour.

The preceding examples indicate that: (1) the use of the working charts to predict the performance of a heat exchanger installed on an engine having a much higher compressor-pressure ratio, and consequently a lower engine-temperature ratio, than that assumed for the hypothetical

engine would give results that were optimistic; and (2) the effect of a change in corrected engine gas flow per unit of tail-pipe area on predicted heat-exchanger performance is very slight. Inasmuch as there is not likely to be an appreciable increase in corrected engine gas flow per unit of tail-pipe area, the use of the working charts to predict the performance of heat exchangers installed on high pressure-ratio engines will give optimistic results.

METHOD OF DETERMINING EFFECT OF HEAT EXCHANGER ON ENGINE PERFORMANCE

The application of a tail-pipe heat exchanger to a turbojet engine introduces an engine cycle loss and a pumping loss, both of which depreciate the engine performance. The cycle loss arises because the removal of energy from the tail pipe lowers the total temperature at the jet and thereby decreases the jet thrust of the engine. The pumping loss results from the extraction of power from the engine to force the air through the air side of the heat exchanger. This power extraction may detract directly from the engine performance (shaft-power extraction and an auxiliary blower) or may decrease the propulsive effort even though the engine net thrust is unaffected (inlet-momentum drag for a ram-operated exchanger).

The pumping characteristics (the relation between the engine total-pressure ratio P_3/P_1 and engine total-temperature ratio T_3/T_1) of the turbojet engine are unaffected by the extraction of heat by means of a tail-pipe heat exchanger because the heat extraction occurs downstream of the basic turbojet engine. However, the extraction of heat from the tail-pipe gas decreases the tail-pipe temperature ratio T_5/T_3. Accompanying this decrease in tail-pipe temperature ratio is a slight momentum-pressure increase (the inverse of the momentum-pressure loss accompanying heat addition, as in tail-pipe burning); this increase is so slight, however, with the normal velocities in the engine tail pipe, that it can be neglected in the calculation of engine performance.

The engine cycle performance with a tail-pipe heat exchanger is given in figures 6 to 9 for a ram pressure ratio of 1.35, corrected engine speeds of 0.9, 1.0, and 1.1 times the rated value, and tail-pipe total-temperature ratios of 1.00 (no heat extracted), 0.99, 0.98, and 0.97. These data were computed by the method used in reference 6 to determine the performance of a tail-pipe burner. The results of heat balance calculations presented in figure 6 relate the heat-removal factor (the corrected heat removed per pound of corrected thrust at rated engine operation $\frac{q/\delta_1\sqrt{\theta_1}}{(F_n/\delta_1)_R}$) to the fraction of rated

corrected thrust $\frac{F_n/\delta_1}{(F_n/\delta_1)_R}$, the tail-pipe temperature ratio T_5/T_3, and the corrected engine speed. Inasmuch as the turbine-outlet temperature is affected by changes in thrust level the heat-removal factor varies directly with both T_5/T_3 and $\frac{F_n/\delta_1}{(F_n/\delta_1)_R}$. Because the turbine-outlet temperature is relatively unaffected by changes in corrected engine speed within the range shown, the heat-removal factor at a given thrust level is relatively unaffected by changes in engine speed.

In figures 7 and 8, respectively, the fraction of rated engine temperature ratio $\frac{T_3/T_1}{(T_3/T_1)_R}$ and the fraction of rated tail-pipe nozzle area $\frac{A_5}{(A_5)_R}$ are given as functions of the corrected thrust, corrected engine speed, and the tail-pipe temperature ratio. The effect on engine thrust of heat extraction at constant turbine-outlet (and hence turbine-inlet) temperature can be determined from figure 7, and the effect of heat extraction with constant tail-pipe nozzle area can be obtained from figure 8. A comparison of the spread of the curves with heat extraction (that is, with variation in T_5/T_3) indicates that the effect of heat extraction on net thrust at a constant corrected engine speed is roughly three times as great for constant-area operation as for constant-temperature operation. This larger thrust decrease with constant-area operation results from a decrease in turbine-inlet temperature necessary in order to prevent the engine speed from increasing when the tail-pipe pressure is lowered as a result of the higher gas density at the tail-pipe nozzle when heat is extracted.

The effect of tail-pipe heat extraction on the thrust specific fuel consumption is shown in figure 9. These curves are applicable to any mode of engine operation.

Although figures 6 to 9 are for a ram pressure ratio of 1.35 (Mach number of approximately 0.7) they can be used for Mach numbers from 0.5 to 0.9 with an error of less than 4 percent.

As mentioned earlier, an additional propulsive thrust loss is necessary in order to force the air through the air side of the heat exchanger. The over-all effect of heat extraction with a tail-pipe heat exchanger therefore requires the evaluation of this loss as well as the engine cycle loss.

DETERMINATION OF UNFINNED HEAT-EXCHANGER PERFORMANCE

It is assumed that in the usual heat-exchanger design problem the engine tail-pipe diameter will be fixed by the particular type of engine

installed in the airplane and that the heat-exchanger length will be governed by space limitations of the engine installation. The problem then will be to determine the amount of heat which can be extracted from the heat exchanger at the flight conditions of interest and to establish the proper combination of annular passage height, outlet-air temperature, and rate of air flow through the annulus. In addition, it is necessary to determine the pressure drop on the air side of the heat exchanger and to determine the effect of heat-exchanger operation on engine performance.

The detailed procedure for using the generalized working charts (figs. 4 and 5) to design a tail-pipe heat exchanger and the use of figures 6 to 9 to determine the effect of the heat exchanger on engine performance will now be illustrated.

As indicated previously, it is assumed that the engine tail-pipe diameter, heat-exchanger length, and flight conditions are known. For a given value of heat-exchanger outlet-air temperature, several values of heat output q are assumed and the parameters $\frac{q}{D\mathcal{l}\sqrt{\theta_1}}$ and $\frac{W_a}{D\mathcal{l}}$ $\left(\text{where } \frac{W_a}{D\mathcal{l}} = \frac{\frac{q}{D\mathcal{l}}}{c_{p,a}(T_7-T_1)}\right)$ are then computed. From the applicable generalized working chart the value of $\mathcal{l}^{0.8}/y$ (corresponding to the values of $\frac{q}{D\mathcal{l}\sqrt{\theta_1}}$ and $\frac{W_a}{D\mathcal{l}}$ computed for each assumed value of heat output) is obtained and the heat-exchanger passage height y is computed. With the passage height and air flow known, the pressure drop through the annular passage and consequently the ratio of the total pressure at the outlet to the total pressure at the inlet of the air side of the heat exchanger P_7/P_6 can be determined. In the present example a simplified method (considering friction and momentum pressure losses separately) was used to determine the pressure drop on the air side of the heat exchanger.

The effect on engine performance of heat extraction from the tail-pipe gas can be determined from figures 6 to 9 in the following manner. With the flight and engine-operating conditions known and with the values of heat output previously assumed, the parameters $\frac{F_n/\delta_1}{(F_n/\delta_1)_R}$, $\frac{N/\sqrt{\theta_1}}{(N/\sqrt{\theta_1})_R}$, and $\frac{q/\delta_1\sqrt{\theta_1}}{(F_n/\delta_1)_R}$ are determined. With the use of these values, the tail-pipe temperature ratio T_5/T_3 is obtained from figure 6, and the decrease in net thrust is then determined from figure 7 for the general case or from figure 8 for constant-area operation. The specific fuel consumption is obtained from figure 9.

The results of such calculations (with the exception of specific fuel consumption) for a 6-foot-long heat exchanger installed on a hypothetical engine, the characteristics of which were presented previously, having a tail pipe 2.17 feet in diameter and a rated engine gas flow of 147 pounds per second are presented in figure 10. The heat-exchanger performance at outlet air temperatures ranging from 800° to 1100° R presented in figure 10(a) is for climb operation at a flight Mach number of 0.5 and an altitude of 15,000 feet. The results of calculations for cruise operation at a flight Mach number of 0.7 and an altitude of 30,000 feet are presented in figure 10(b) for outlet air temperatures ranging from 700° to 1000° R.

DISCUSSION OF UNFINNED HEAT-EXCHANGER PERFORMANCE

The results presented in figure 10 indicate that the annular passage height decreases and the pressure drop across the air side of the heat exchanger increases with increase in either heat output or outlet air temperature. The ratio of outlet- to inlet-air pressure on the air side of the heat exchanger is expressed in the charts as P_7/P_6. Figure 10 also indicates that the total loss in net thrust $\Delta F_n/F_n$ varies directly as the heat extracted and as the weight flow through the air side of the heat exchanger.

The minimum heat-exchanger pressure ratio for a ram-operated anti-icing system is shown as a dashed line across the curves of pressure ratio. A ram-operated system is defined as one in which the pressure drop across the air side of the heat exchanger does not exceed one-half the free-stream dynamic pressure, since it is considered that the pressure drop through the ducting of the thermal anti-icing system will approximate that amount (reference 7).

It is evident that at the two respective assumed flight conditions the greatest heat output as limited by heat-exchanger pressure ratio is obtained at the lowest air temperatures investigated. For the climb condition at a flight Mach number of 0.5 at 15,000 feet, figure 10(a) indicates that for a ram-operated heat exchanger 6 feet in length the greatest heat output is 780,000 Btu per hour, with an outlet-air temperature of 800° R and annular passage height of 0.042 foot. At these conditions the loss in net thrust, for constant tail-pipe nozzle area operation, is slightly less than 2 percent. According to figure 10(b), this same heat-exchanger configuration during cruise operation would deliver approximately 425,000 Btu per hour at an outlet air temperature of 700° R with a net thrust loss between 2 and 3 percent.

In order to obtain greater heat outputs than those possible with a ram-operated system, pressures greater than those resulting from ram pressure are necessary to force the required air flow through the

anti-icing system. A first approximation of the pressure required to pump the air through the anti-icing system (including the heat exchanger) is obtained from figure 10 by dividing the limiting heat-exchanger pressure ratio for a ram-operated system by the pressure ratio corresponding to the desired heat output and outlet-air temperature. For example, a heat output of 920,000 Btu per hour is obtainable for an annular passage height of 0.035 foot and outlet-air temperature of 800° R at this assumed flight condition. However, a pressure approximately 11 percent greater than ram pressure is required to pump the air through the anti-icing system.

The total net thrust loss shown in figure 10 is the sum of the cycle loss (at constant nozzle-area operation) and the inlet momentum drag corresponding to the weight flow of air through the heat exchanger. In addition, for portions of the curves to the right of the ram-operating-limit curve, a further thrust loss would result from the power extraction necessary to boost the pressure to the value required. The portion of the thrust loss charged to the pumping of heat-exchanger air is arbitrary, as this loss would depend on the method of attaining the desired air flow and pressure. It should be noted that the ram-operated heat exchanger may not be the optimum as far as thrust loss is concerned, as the energy used to develop the ram pressure rise is obtained from the jet and the jet propulsive efficiency would therefore influence the over-all efficiency of the ram-compression cycle. A decrease in the thrust loss due to pumping the heat-exchanger air flow might result if an auxiliary blower system were used to compress boundary-layer air to the desired pressure.

COMPARISON OF FINNED AND UNFINNED HEAT-EXCHANGER PERFORMANCE

For purposes of comparison calculations of the performance of finned and unfinned heat exchangers were made assuming a tail-pipe diameter of 2.17 feet and the heat-exchanger inlet-air temperature equal to ram-air temperature. It was also assumed that the fin spacing in the finned heat exchanger was equal to the passage height, the fin thickness was 1/32 inch, and the fin material had a thermal conductivity of 9 Btu/(hr)(ft)(°F) (typical of high-temperature materials). The results of calculations comparing the lengths of finned and unfinned heat exchangers having equal passage height and designed to deliver the same heat output at an outlet-air temperature of 800° R, flight Mach number of 0.5, and an altitude of 15,000 feet are presented in figure 11.

Figure 11 shows that, for equal passage height and heat output, the finned heat exchanger has a shorter length than the unfinned type. However, it should be noted that this advantage for the finned heat exchanger becomes appreciable only at the lower range of heat output, since the length ratio l_f/l_u increases rapidly with increasing heat output.

Similar trends in the performance comparison were observed at higher outlet-air temperatures. It was found that for a given unfinned heat-exchanger length and heat output, the length ratio l_f/l_u decreased with an increase in the heat-exchanger outlet-air temperature. This effect, however, was accompanied by a decrease in passage height. It has already been shown, in the discussion of heat-exchanger performance, that pressure drop increased with increasing outlet air temperature for constant length, because of the decreasing passage height. Thus it is evident that the selection of a low outlet-air temperature is favorable to the finned as well as unfinned type heat exchangers.

In examining the merits of adding fins to the air side of tailpipe heat exchangers it is of interest to make two types of comparison. The first of these is for the case of equal length, passage height, and outlet-air temperature; the second comparison is for the case of equal pressure drop through the air side of the heat exchanger, equal length, and outlet-air temperature.

Pressure drop is very important in both cases. The friction loss, which is most critical in this problem (effect of fins on the momentum loss is small since outlet-air temperature is held constant), is proportional to the ratio of length to hydraulic diameter. For the case of equal passage height and with fin spacing equal to fin height, the l/D_h ratio, and thus the friction pressure drop in a finned passage, is about double that of an unfinned passage.

The performance of finned and unfinned heat exchangers of equal length (6 ft) and diameter (2.17 ft) and operating at an outlet-air temperature of 800° R is given in figure 12 for a flight Mach number of 0.5 and an altitude of 15,000 feet. Figure 12 indicates that for a passage height of 0.042 foot the addition of fins to the air side results in an increase in heat output from 780,000 to 875,000 Btu per hour. However, the pressure drop through the air side of the heat exchanger is approximately 2.7 times that of the unfinned heat exchanger. Because of the greater pressure drop, the finned heat exchanger requires a pressure about 15 percent greater than the free-stream pressure, whereas the unfinned heat exchanger is ram-operated.

According to figure 12, an unfinned heat exchanger 6 feet in length operating at an outlet-air temperature of 800° R and a pressure ratio of 0.80 (a condition requiring a pressure approximately 15 percent greater than that obtainable with ram pressure) has an annulus passage height of 0.034 foot and heat output of 950,000 Btu per hour. Thus for a heat-exchanger pressure ratio of 0.80 (equal pressure drop through the air side of both heat exchangers), the unfinned heat exchanger has a heat output approximately 8 percent greater than that of the comparable finned heat exchanger.

This comparison (at operating conditions requiring a pressure greater than that obtainable with ram pressure) indicates that, in order to realize equal pressure drop through the air side, the passage height of a finned heat exchanger must be greater than that of an unfinned heat exchanger and that this requirement eliminates the gain in heat output afforded by the addition of fins. Consequently where high heat outputs are required the unfinned heat exchanger because of its lighter weight and simpler construction probably would be preferable to the finned type.

CONCLUDING REMARKS

The performance of parallel-flow-type unfinned tail-pipe heat exchangers can be determined by the method presented herein. The results of this analysis are presented in the form of generalized working charts that are applicable to a wide range of flight conditions. The performance of unfinned tail-pipe heat exchangers installed on nonafterburning engines having a nominal compressor pressure ratio of 4.0, rated engine temperature ratio of 3.4, and rated corrected gas flow per unit of tail-pipe area of approximately 40 pounds per second per square foot can be determined by use of these charts. The use of these working charts to predict the performance of heat exchangers installed on engines having higher compressor pressure ratios (and consequently rated engine-temperature ratios less than 3.4) will give results that are optimistic. The method of calculating heat-exchanger performance as set forth in this analysis, however, is still applicable.

The results presented herein indicate that at a flight Mach number of 0.5 and an altitude of 15,000 feet a 6-foot-long ram-operated heat exchanger installed on a nonafterburning turbojet engine (tail-pipe diameter, 2.17 ft. rated corrected gas flow per unit of tail-pipe area, 40 lb/(sec)(sq ft); rated engine temperature ratio, 3.4) has a heat output of approximately 780,000 Btu per hour. This heat output is obtained with a heat-exchanger outlet-air temperature of 800° R. At these conditions the over-all effect on engine performance is a reduction in net thrust of the order of 2 percent. Higher heat outputs are obtainable with parallel-flow-type heat exchangers if a greater weight flow of air is pumped through the air side of the heat exchanger. For this mode of operation, the reduction in propulsive thrust would be somewhat greater than for the ram-operated case.

Comparison of the performance of finned and unfinned heat exchangers on the basis of equal pressure drop through the air side at high heat outputs indicates that the unfinned parallel-flow-type tail-pipe heat exchanger because of its lighter weight and simpler construction is probably preferable to the longitudinally finned heat exchanger.

Lewis Flight Propulsion Laboratory,
National Advisory Committee for Aeronautics,
Cleveland, Ohio, May 16, 1951.

APPENDIX

DERIVATION OF RELATION BETWEEN PARAMETER $\frac{W_a c_{p,a}}{US}$ AND FLUID TEMPERATURES

Under steady-state conditions, the rate of heat transfer from the exhaust gas through a thin separating wall to the air flowing over the outer surface of the tail pipe is given by (see sketch)

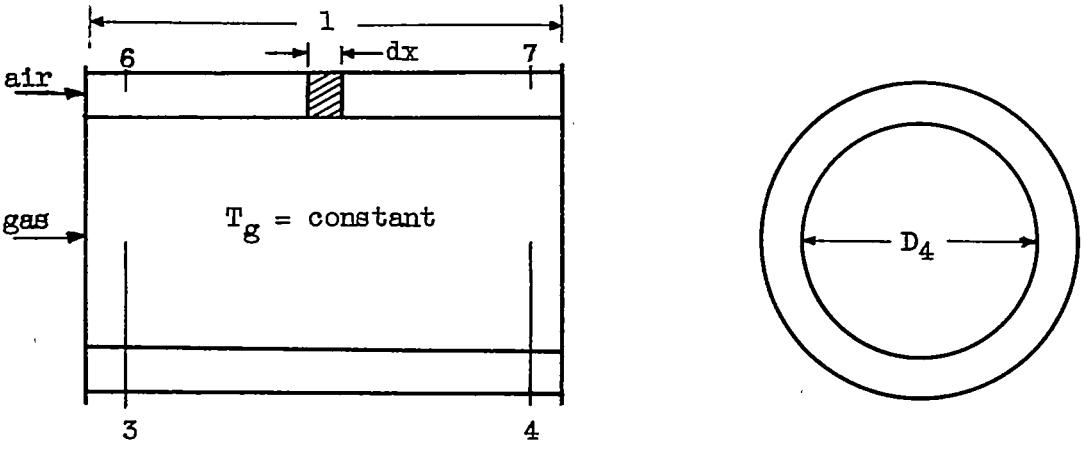

$$W_a c_{p,a}\, dT_a = U\pi D_4 (T_g - T_a)\, dx \tag{A1}$$

$$\frac{dT_a}{(T_g - T_a)} = \frac{U\pi D_4 dx}{W_a c_{p,a}} \tag{A2}$$

After integration

$$-\ln(T_g - T_a) = \frac{U\pi D_4 x}{W_a c_{p,a}} + C_1 \tag{A3}$$

$$T_g - T_a = C_2 e^{-\left(\frac{U\pi D_4 x}{W_a c_{p,a}}\right)} \tag{A4}$$

and when $x = 0$, $T_g = T_3$, and $T_a = T_6$,

$$C_2 = T_3 - T_6 \tag{A5}$$

Substitution of equation (A5) in equation (A4) gives

$$T_g - T_a = (T_3 - T_6)e^{-\left(\frac{U\pi D_4 x}{W_a c_{p,a}}\right)} \tag{A6}$$

When $x = l$, then $\pi D_4 l = S$

$$T_4 - T_7 = (T_3 - T_6)e^{-\left(\frac{US}{W_a c_{p,a}}\right)} \tag{A7}$$

but

$$T_7 - T_1 = (T_4 - T_1) - (T_4 - T_7) \tag{A8}$$

or

$$T_4 - T_7 = T_4 - T_1 - (T_7 - T_1) \tag{A9}$$

Substituting equation (A9) in equation (A7) yields

$$(T_4 - T_1) - (T_7 - T_1) = (T_3 - T_6)e^{-\left(\frac{US}{W_a c_{p,a}}\right)} \tag{A10}$$

If equation (A10) is rearranged and divided by $(T_3 - T_1)$,

$$\frac{T_7 - T_1}{T_3 - T_1} = \frac{T_4 - T_1}{T_3 - T_1} - \left(\frac{T_3 - T_6}{T_3 - T_1}\right)e^{-\left(\frac{US}{W_a c_{p,a}}\right)} \tag{A11}$$

but $T_4 = T_3$; therefore,

$$\frac{\frac{T_7}{T_1} - 1}{\frac{T_3}{T_1} - 1} = 1 - \left(\frac{\frac{T_3}{T_1} - \frac{T_6}{T_1}}{\frac{T_3}{T_1} - 1}\right)e^{-\left(\frac{US}{W_a c_{p,a}}\right)} \tag{A12}$$

REFERENCES

1. Hensley, Reece V., Rom, Frank E., and Koutz, Stanley L.: Effect of Heat and Power Extraction on Turbojet-Engine Performance. I - Analytical Method of Performance Evaluation with Compressor-Outlet Air Bleed. NACA TN 2053, 1950.

2. Rom, Frank E., and Koutz, Stanley L.: Effect of Heat and Power Extraction on Turbojet-Engine Performance. II - Effect of Compressor-Outlet Air Bleed for Specific Modes of Engine Operation. NACA TN 2166, 1950.

3. Koutz, Stanley L., Hensley, Reece V., and Rom, Frank E.: Effect of Heat and Power Extraction on Turbojet-Engine Performance. III - Analytical Determination of Effects of Shaft-Power Extraction. NACA TN 2202, 1950.

4. Koutz, Stanley L.: Effect of Heat and Power Extraction on Turbojet-Engine Performance. IV - Analytical Determination of Effects of Hot-Gas Bleed. NACA TN 2304, 1951.

5. Boelter, L.M.K., Martinelli, R.C., Romie, F.E., and Morrin, E.H.: An Investigation of Aircraft Heaters. XVIII - A Design Manual for Exhaust Gas and Air Heat Exchangers. NACA ARR 5A06, 1945.

6. Sanders, Newell D., and Behun, Michael: Generalization of Turbojet-Engine Performance in Terms of Pumping Characteristics. NACA TN 1927, 1949.

7. Jackson, Richard: An Investigation of a Thermal Ice-Prevention System for a C-46 Cargo Airplane. II - The Design, Construction, and Preliminary Test of the Exhaust-Air Heat Exchanger. NACA ARR 5A03a, 1945.

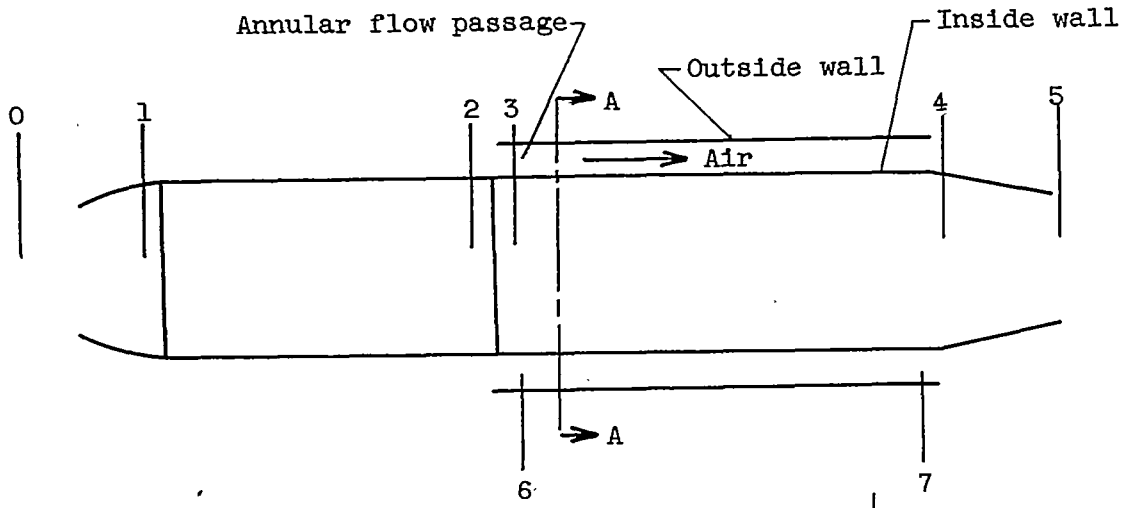

Station

0 Ambient condition

1 Compressor inlet

2 Turbine inlet

3 Turbine outlet

4 Tail-pipe outlet

5 Exhaust-nozzle outlet

6 Heat-exchanger air inlet

7 Heat-exchanger air outlet

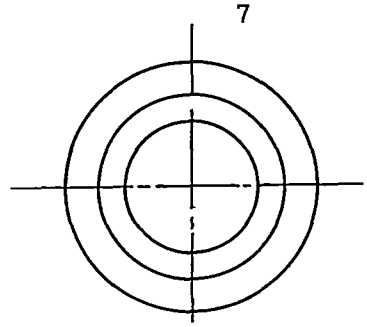

Section A-A

(a) Unfinned heat exchanger.

Figure 1. - Turbojet-engine tail-pipe heat exchanger.

2212

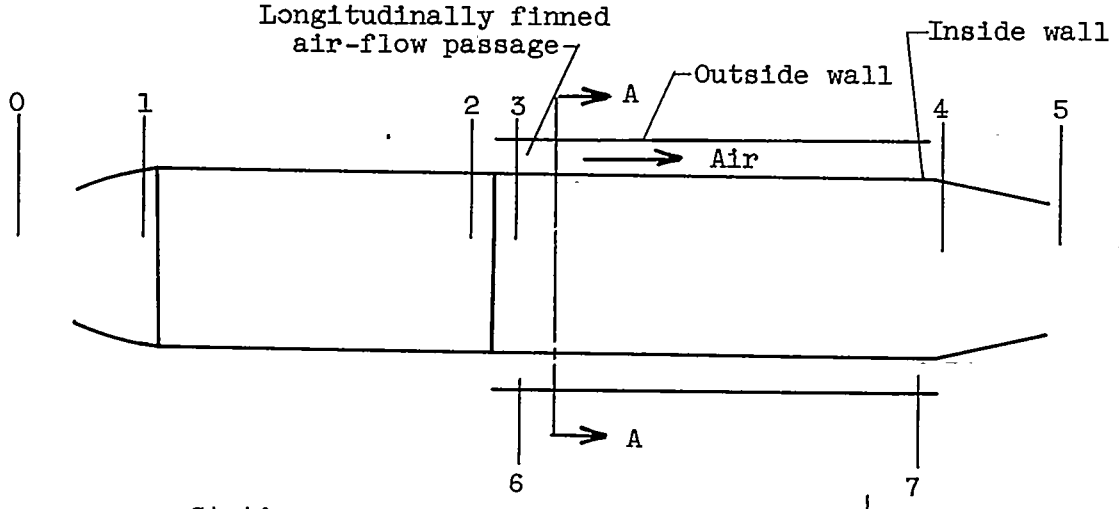

Station

0 Ambient conditions

1 Compressor inlet

2 Turbine inlet

3 Turbine outlet

4 Tail-pipe outlet

5 Exhaust-nozzle outlet

6 Heat-exchanger air inlet

7 Heat-exchanger air outlet

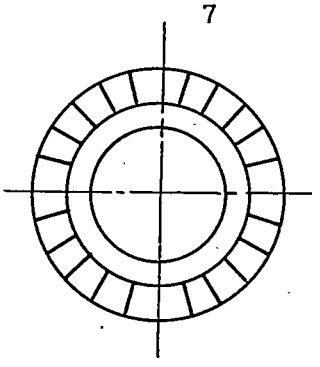

Section A-A

(b) Longitudinally finned heat exchanger.

Figure 1. - Concluded. Turbojet-engine tail-pipe heat exchanger.

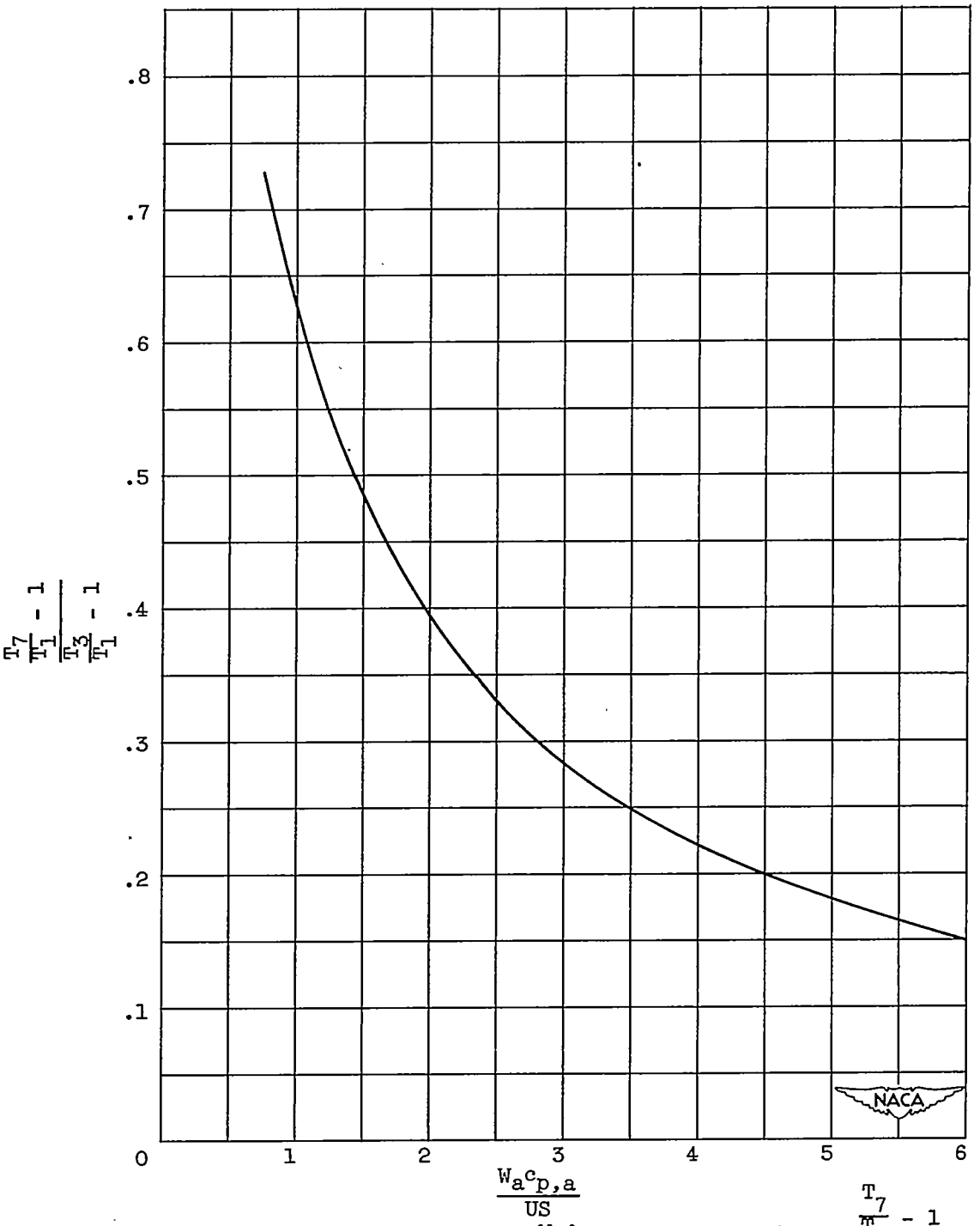

Figure 2. - Variation of parameter $\frac{W_a c_{p,a}}{US}$ with parameter $\frac{\frac{T_7}{T_1} - 1}{\frac{T_3}{T_1} - 1}$.

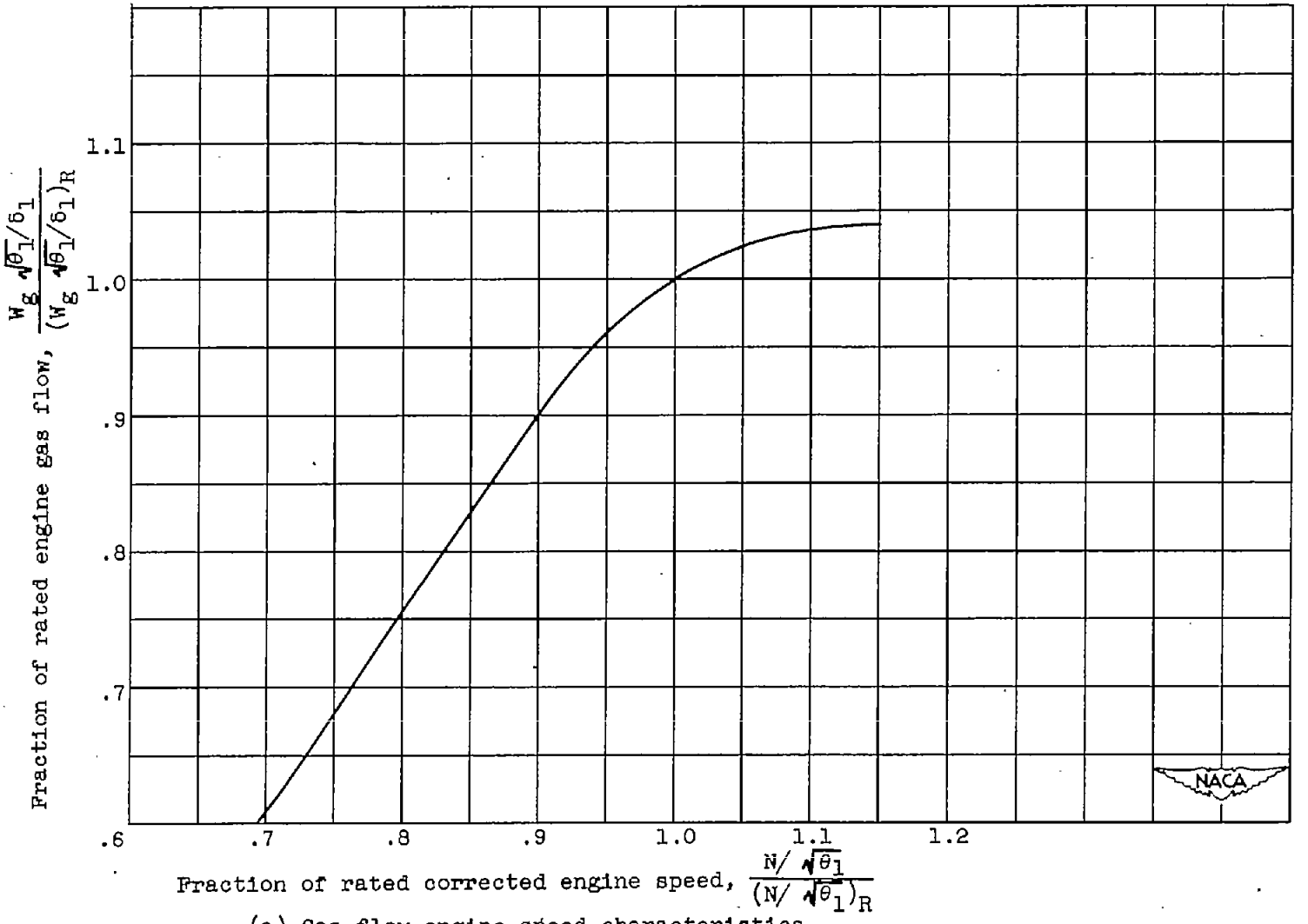

(a) Gas-flow engine-speed characteristics.

Figure 3. - Characteristics of hypothetical turbojet engine.

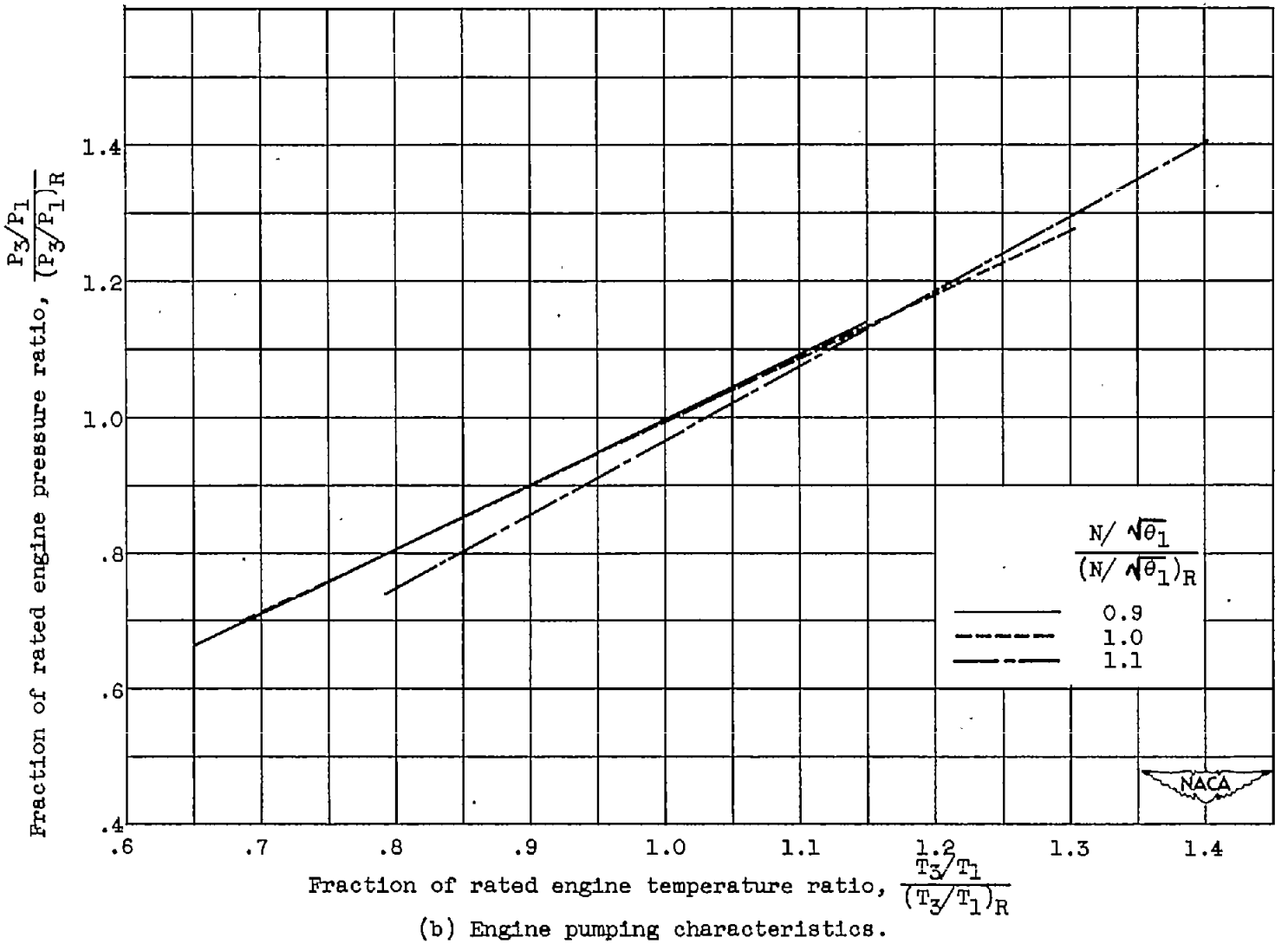

(b) Engine pumping characteristics.

Figure 3. - Concluded. Characteristics of hypothetical turbojet engine.

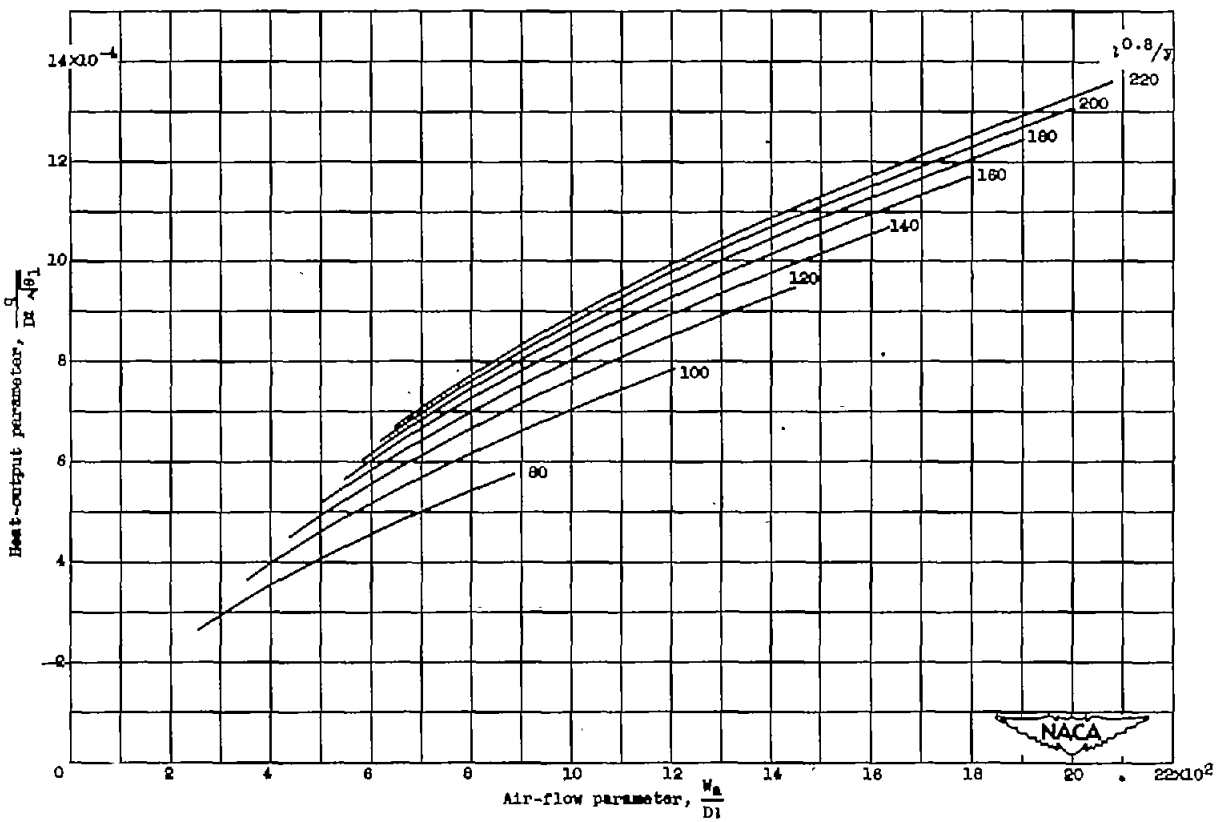

(a) Outlet air temperature, 800° R.

Figure 4. - Characteristics of unfinned tail-pipe heat exchanger during climb condition. Flight Mach number, 0.6; altitude, 5000 to 35,000 feet; engine speed, rated; turbine-inlet temperature, 2000° R.

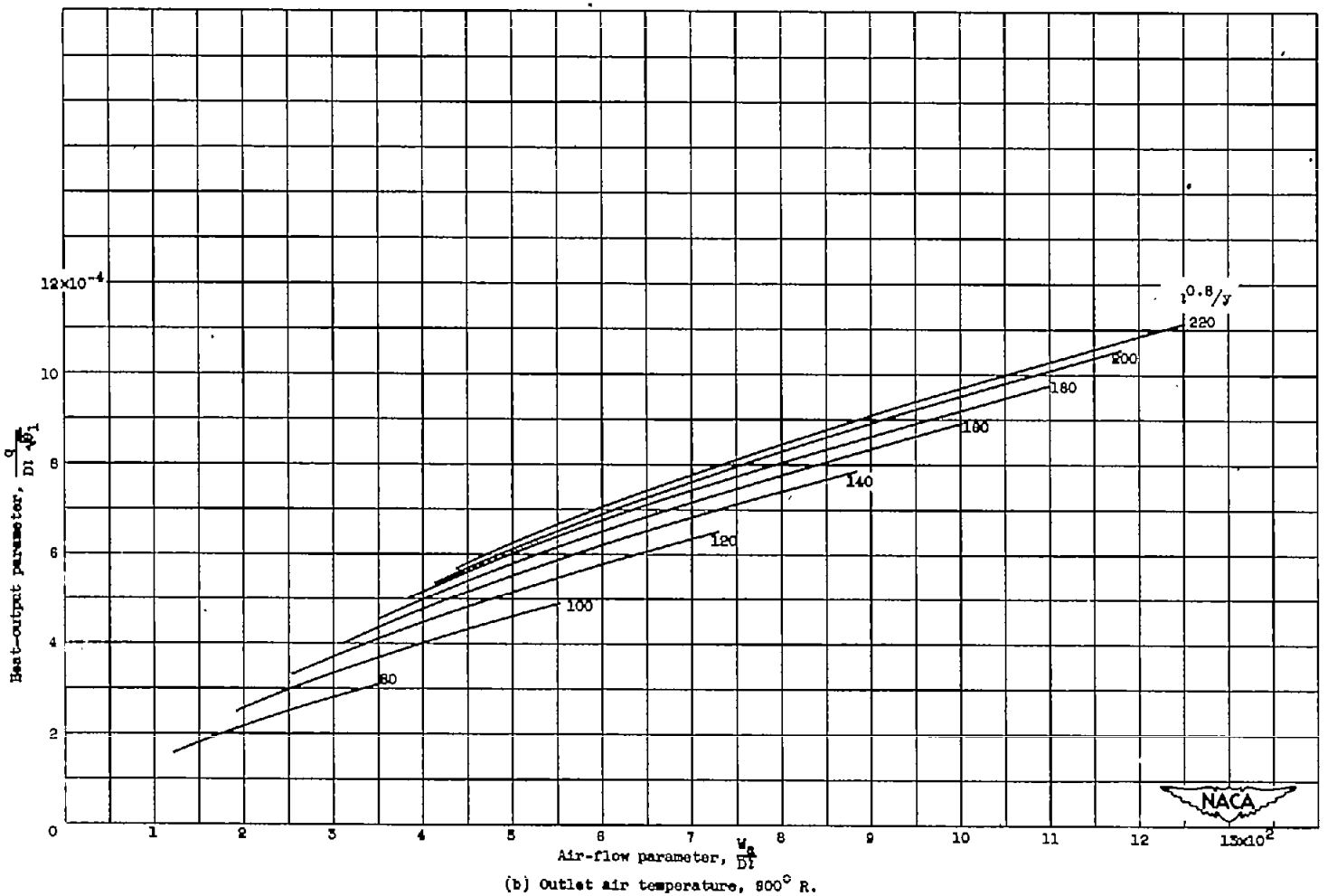

(b) Outlet air temperature, 800° R.

Figure 4. - Continued. Characteristics of unfinned tail-pipe heat exchanger during climb condition. Flight Mach number, 0.6; altitude, 5000 to 35,000 feet; engine speed, rated; turbine-inlet temperature, 2000° R.

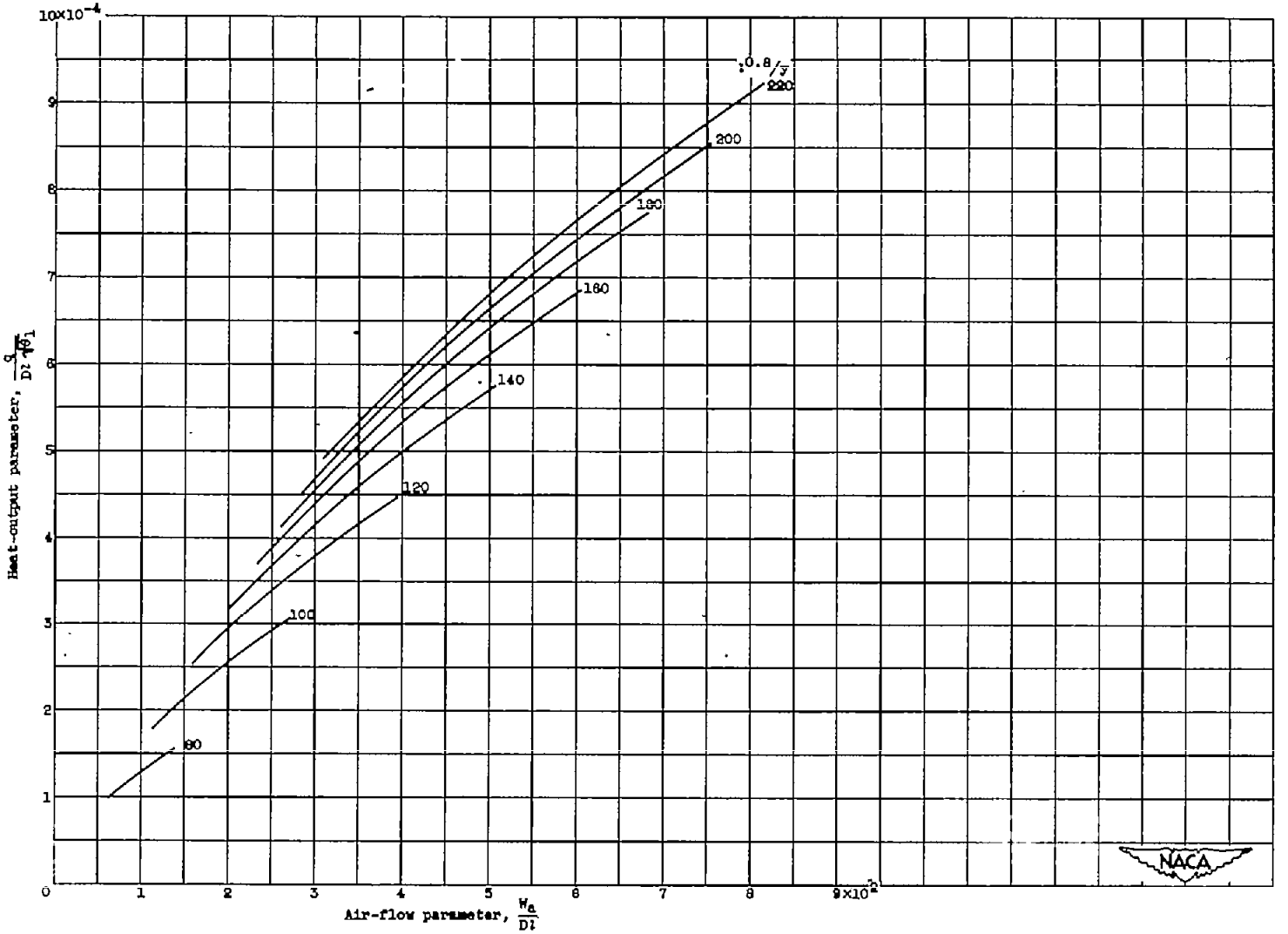

(c) Outlet air temperature, 1000° R.

Figure 4. - Continued. Characteristics of unfinned tail-pipe heat exchanger during climb condition. Flight Mach number, 0.5; altitude, 5000 to 35,000 feet; engine speed, rated; turbine-inlet temperature, 2000° R.

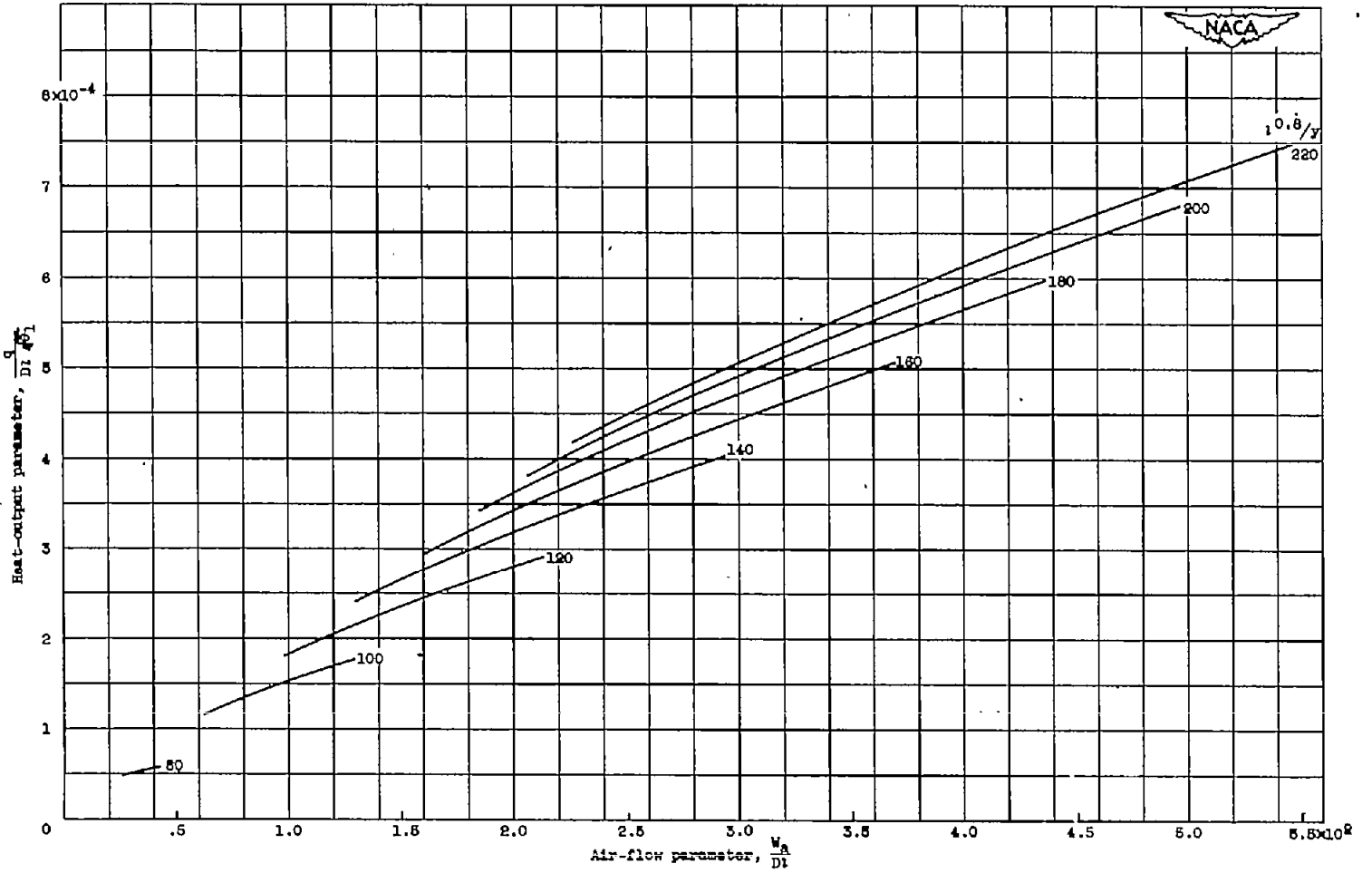

(d) Outlet air temperature, 1100° R.

Figure 4. - Concluded. Characteristics of unfinned tail-pipe heat exchanger during climb condition. Flight Mach number, 0.8; altitude, 5000 to 35,000 feet; engine speed, rated; turbine-inlet temperature, 2000° R.

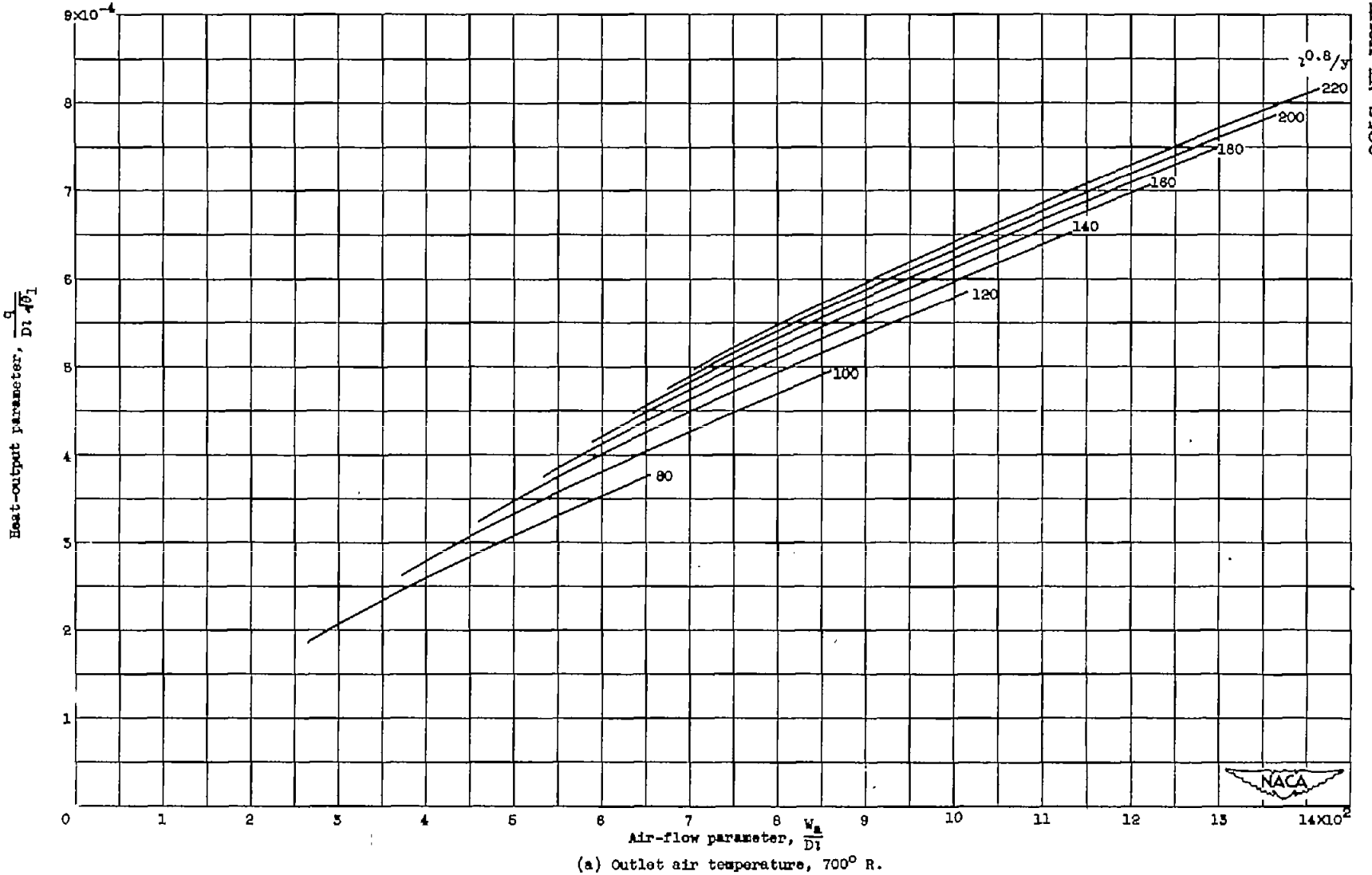

(a) Outlet air temperature, 700° R.

Figure 8. - Characteristics of unfinned tail-pipe heat exchanger during cruise condition. Flight Mach number, 0.7; altitude, 25,000 to 35,000 feet; engine speed and turbine-inlet temperature ratio, 95 percent of rated values.

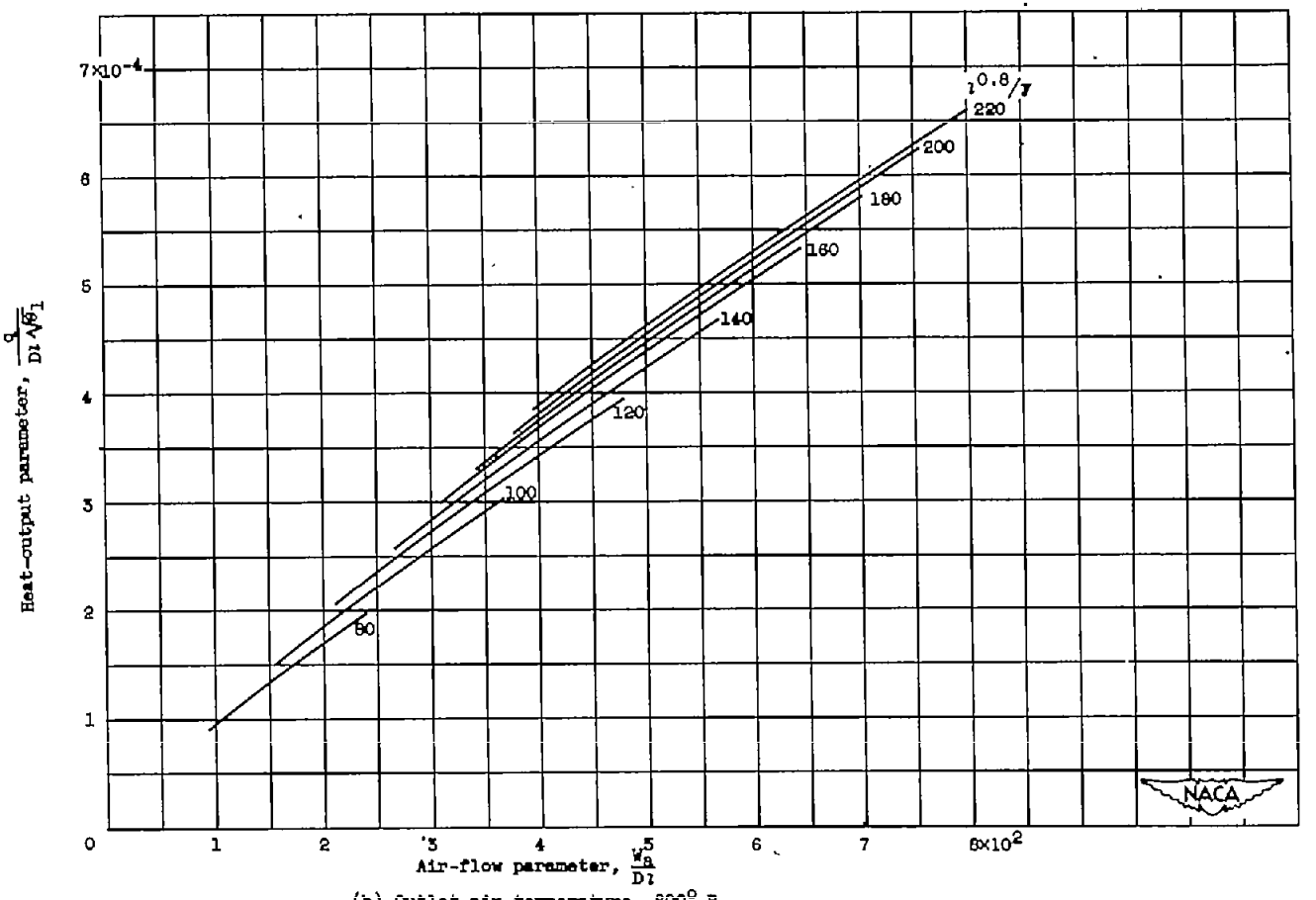

(b) Outlet air temperature, 800° R.

Figure 5. - Continued. Characteristics of unfinned tail-pipe heat exchanger during cruise condition. Flight Mach number, 0.7; altitude, 25,000 to 35,000 feet; engine speed and turbine-inlet temperature ratio, 95 percent of rated values.

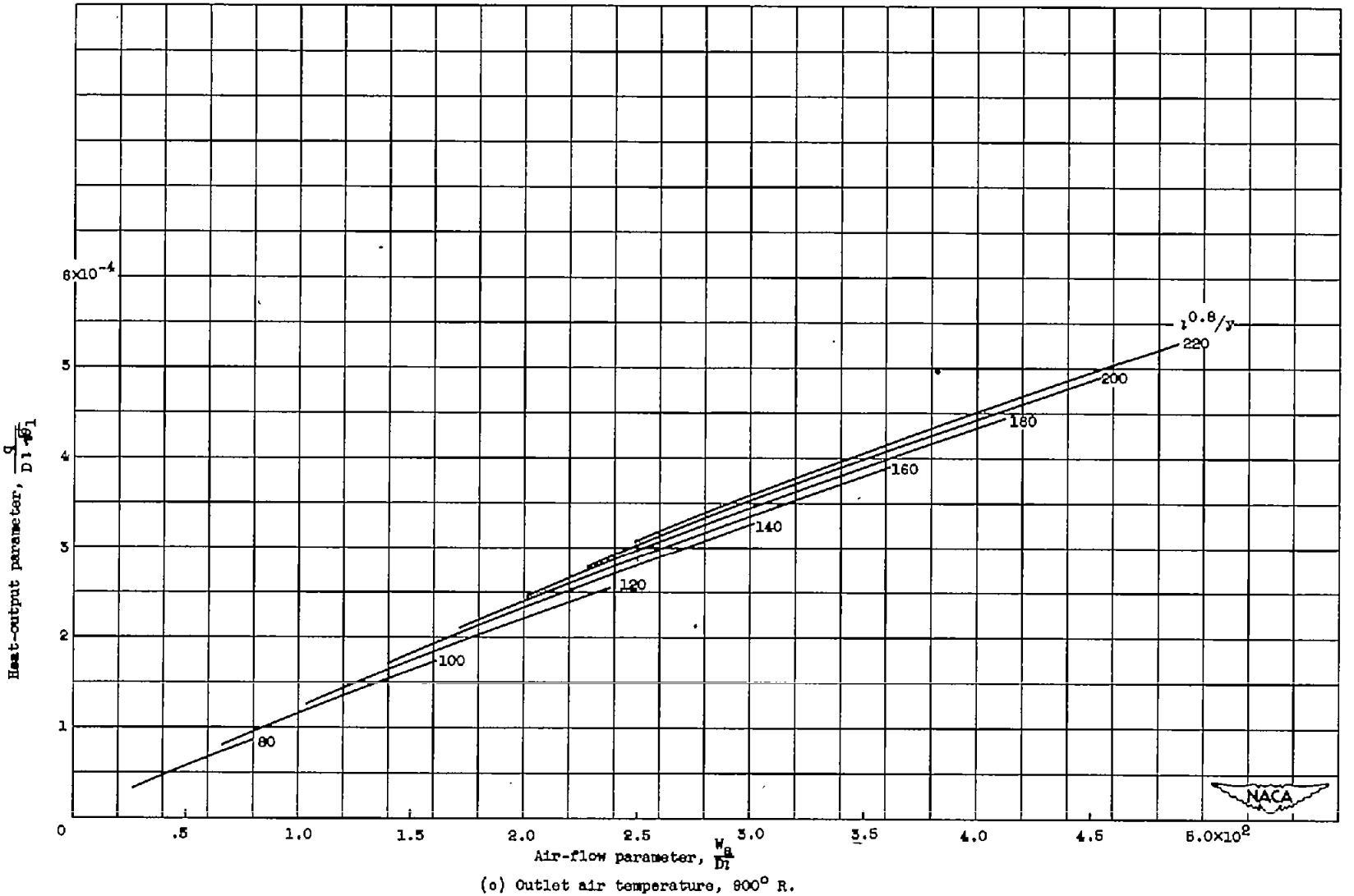

(c) Outlet air temperature, 800° R.

Figure 5. - Continued. Characteristics of unfinned tail-pipe heat exchanger during cruise condition. Flight Mach number, 0.7; altitude 26,000 to 35,000 feet; engine speed and turbine-inlet temperature ratio, 95 percent of rated values.

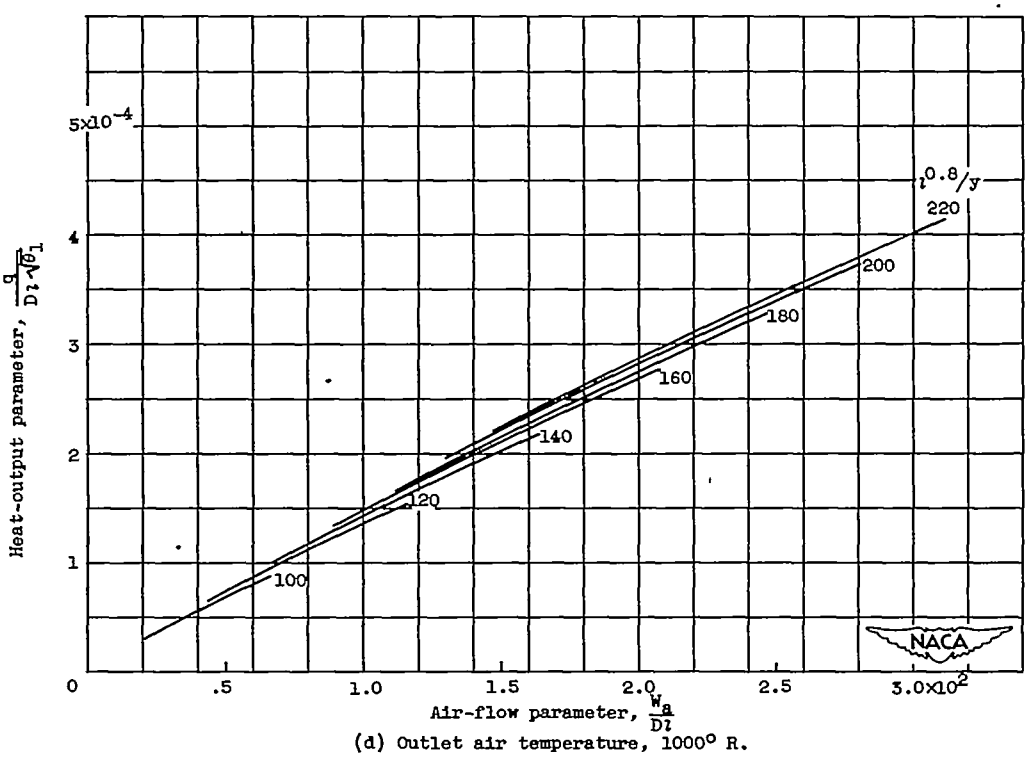

(d) Outlet air temperature, 1000° R.

Figure 5. - Concluded. Characteristics of unfinned tail-pipe heat exchanger during cruise condition. Flight Mach number, 0.7; altitude, 25,000 to 35,000 feet; engine speed and turbine-inlet temperature ratio, 95 percent of rated values.

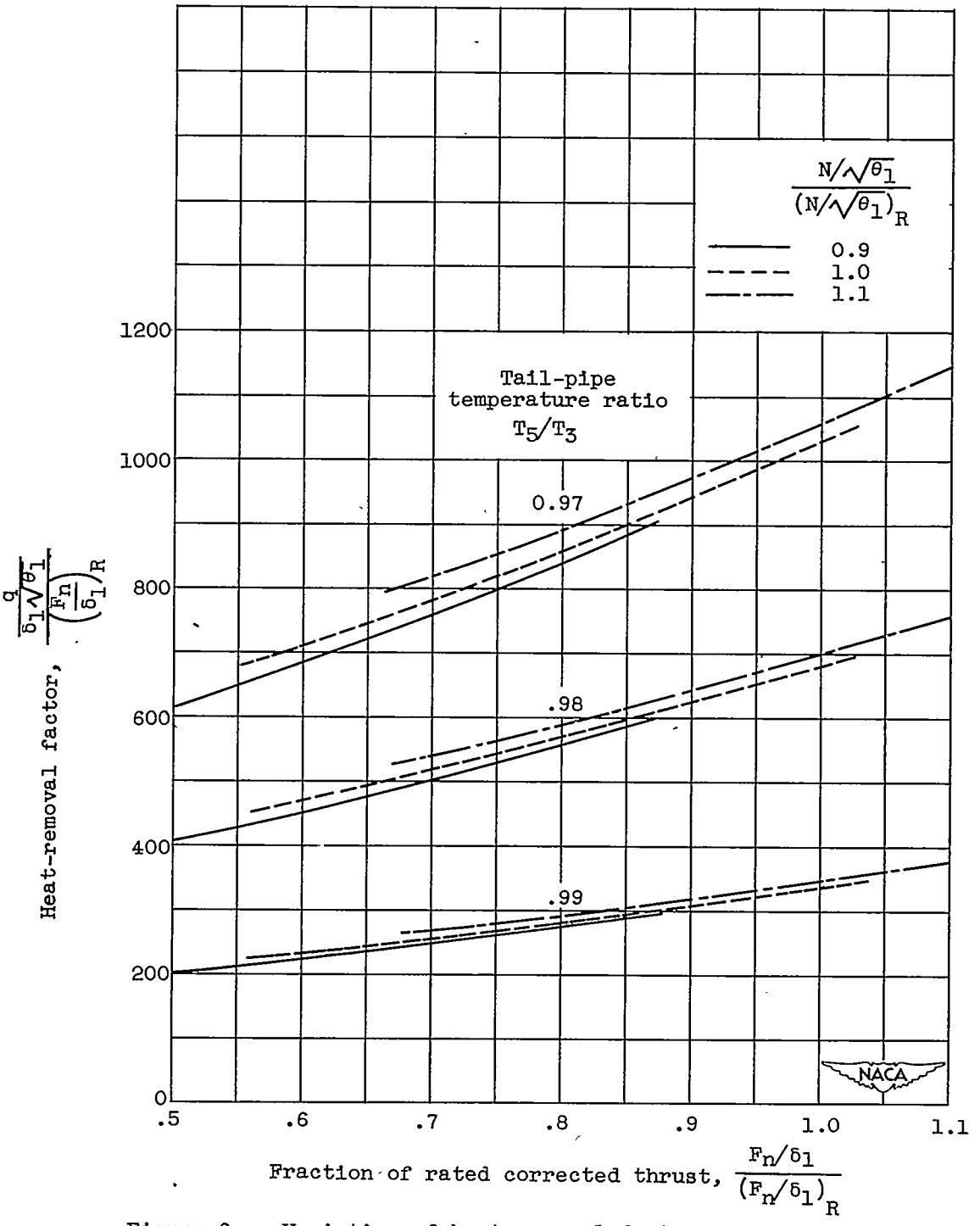

Figure 6. - Variation of heat-removal factor and tail-pipe temperature ratio with engine speed and thrust. Ram pressure ratio, 1.35.

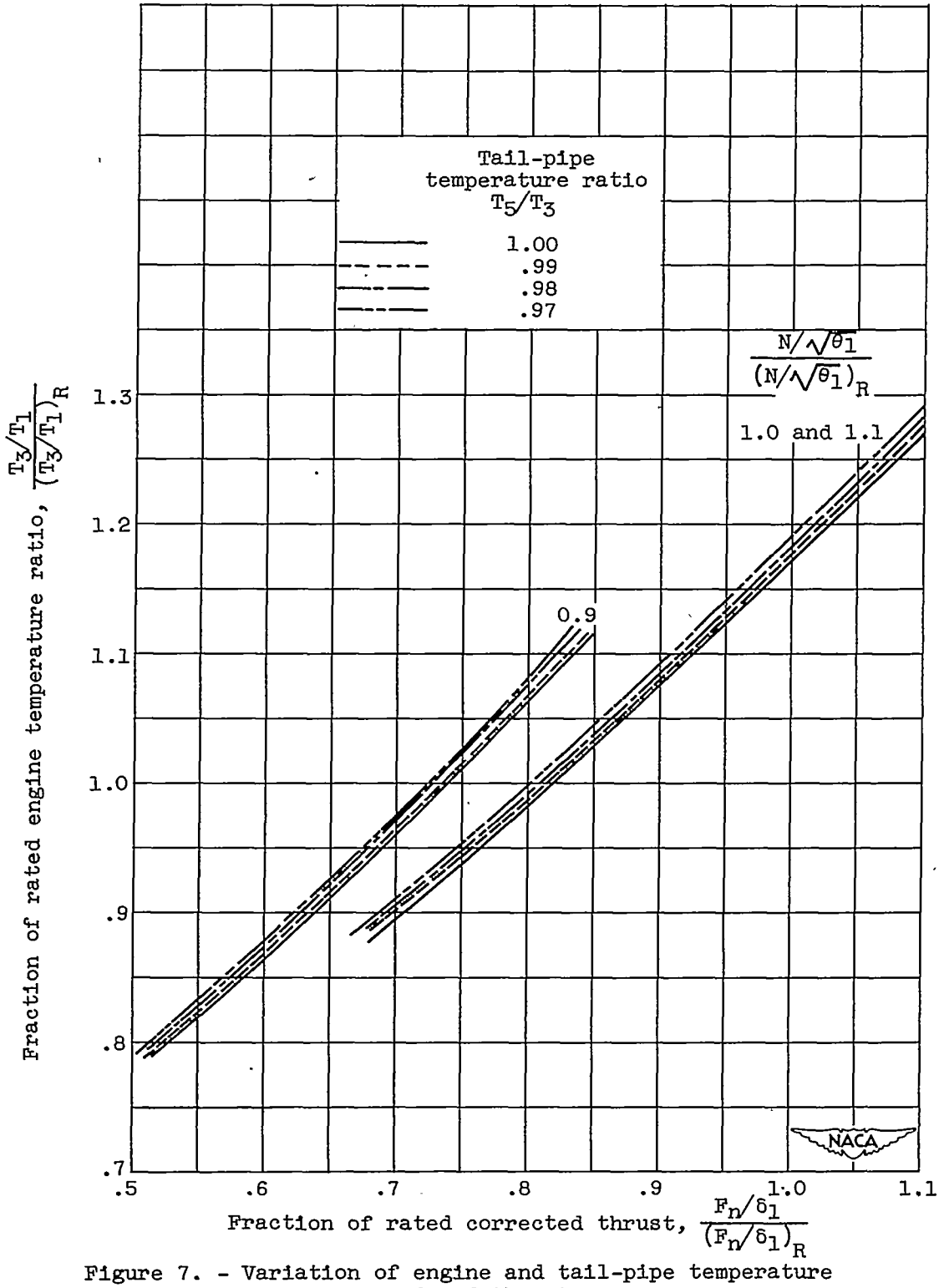

Figure 7. - Variation of engine and tail-pipe temperature ratios with engine speed and thrust. Ram pressure ratio, 1.35.

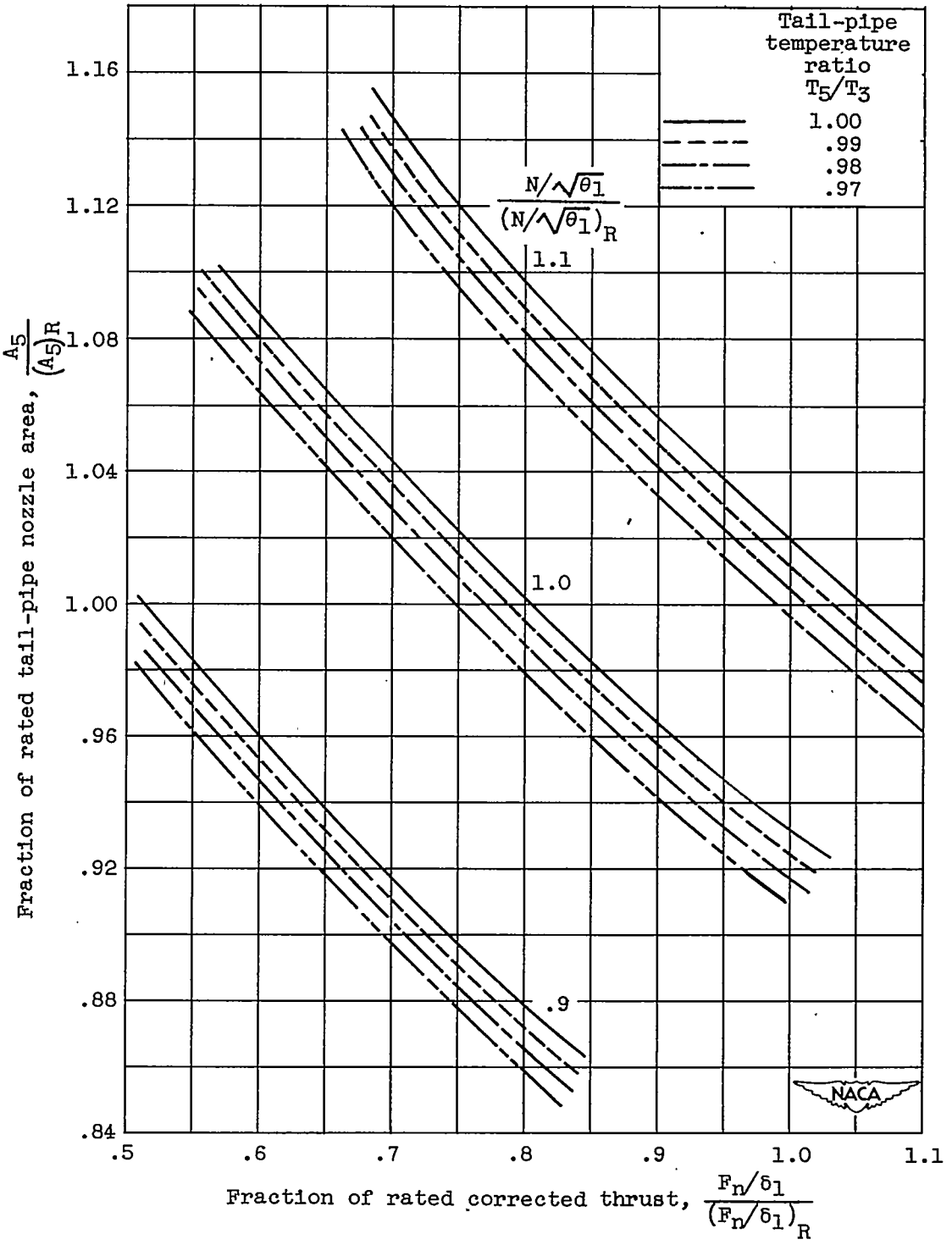

Figure 8. - Variation of tail-pipe nozzle area and temperature ratios with engine speed and thrust. Ram pressure ratio, 1.35.

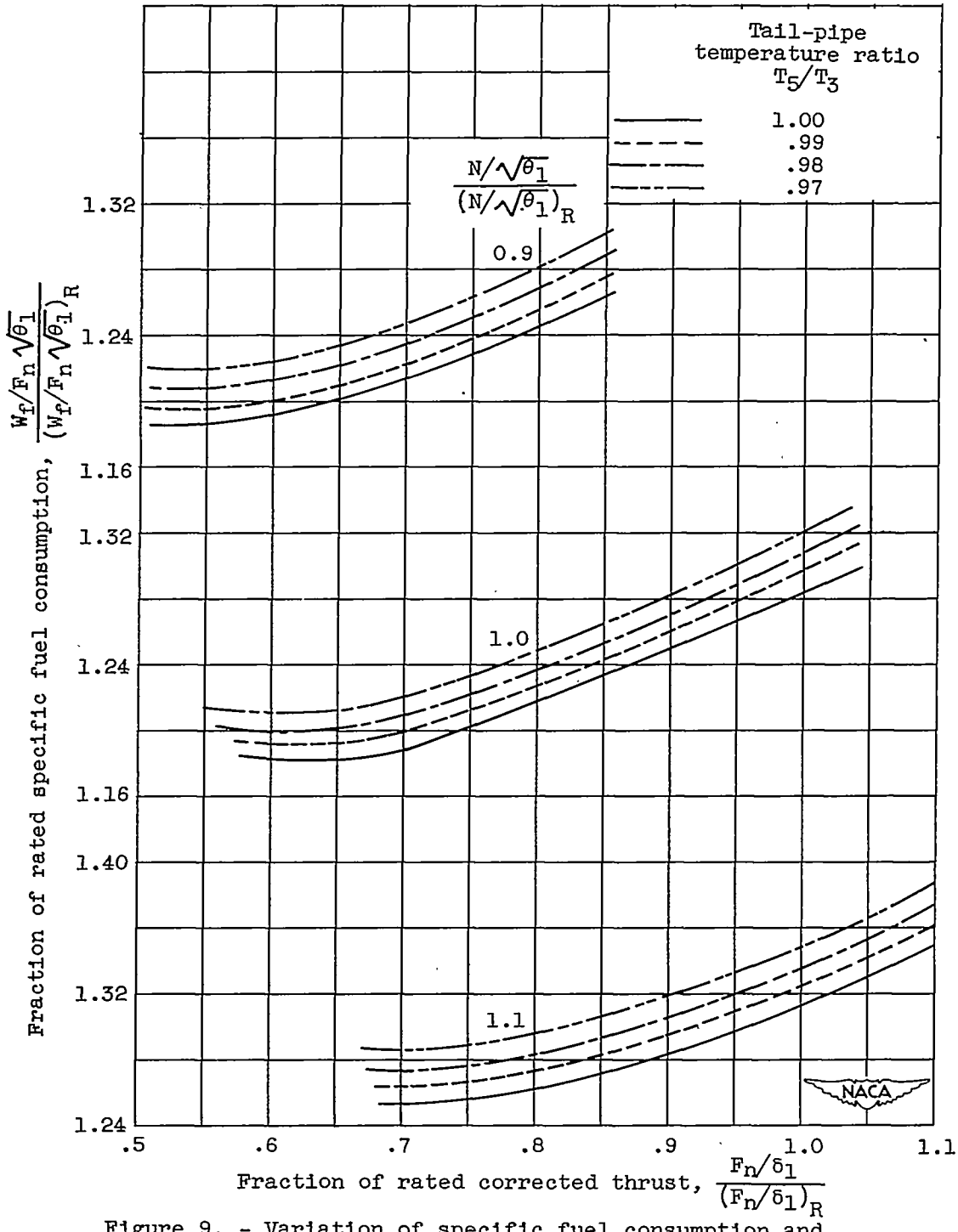

Figure 9. - Variation of specific fuel consumption and tail-pipe temperature ratio with engine speed and thrust. Ram pressure ratio, 1.35.

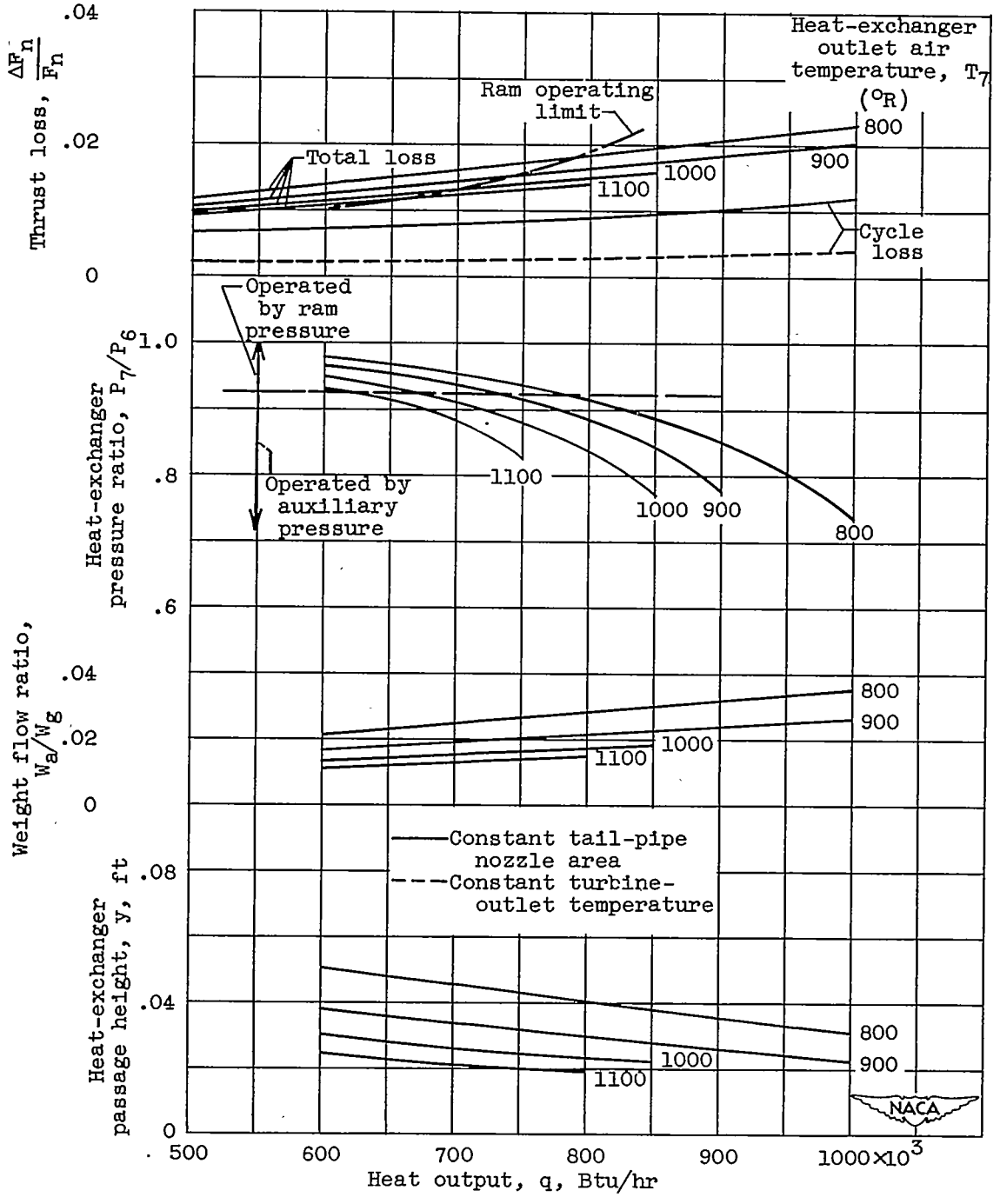

(a) Climb condition: flight Mach number, 0.5; altitude, 15,000 feet.

Figure 10. - Performance of unfinned heat exchanger. Heat-exchanger length, 6 feet; tail-pipe diameter, 2.17 feet; rated engine gas flow, 147 pounds per second.

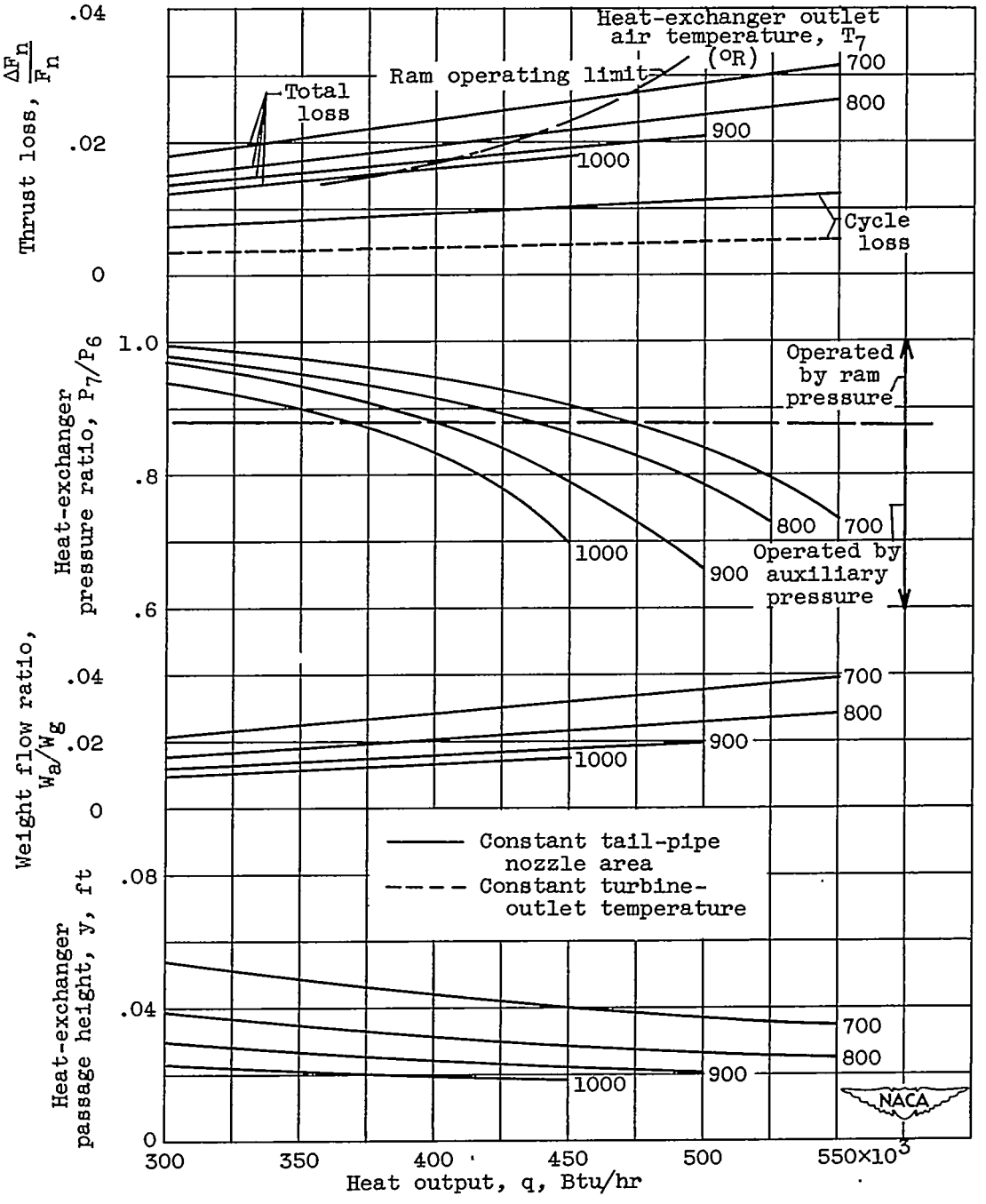

(b) Cruise condition: flight Mach number, 0.7; altitude, 30,000 feet.

Figure 10. - Concluded. Performance of unfinned heat exchanger. Heat-exchanger length, 6 feet; tail-pipe diameter, 2.17 feet; rated engine gas flow, 147 pounds per second.

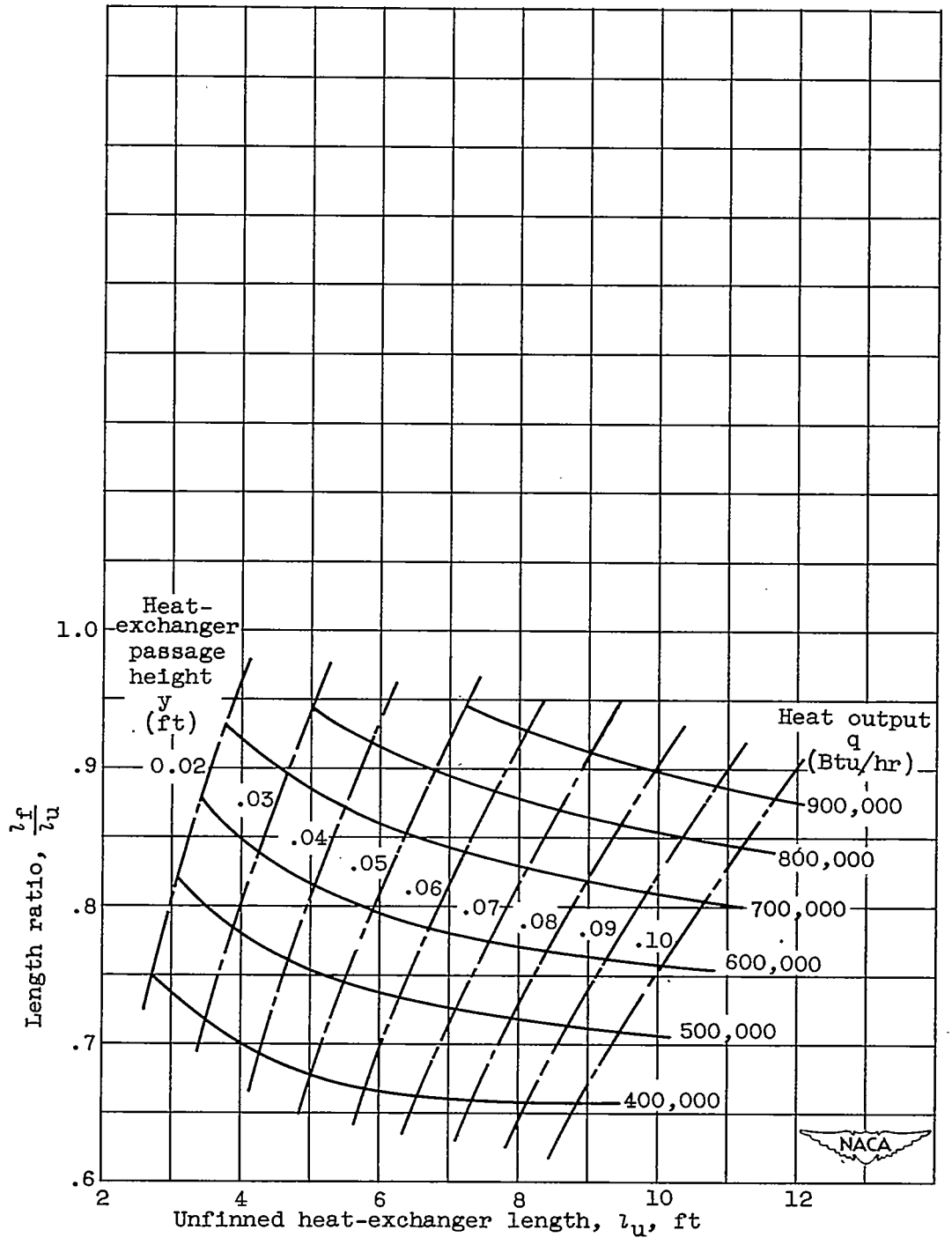

Figure 11. - Comparison of lengths of finned and unfinned heat exchangers. Flight Mach number, 0.5; altitude, 15,000 feet; tail-pipe diameter, 2.17 feet; rated engine gas flow, 147 pounds per second; outlet air temperature, 800° R.

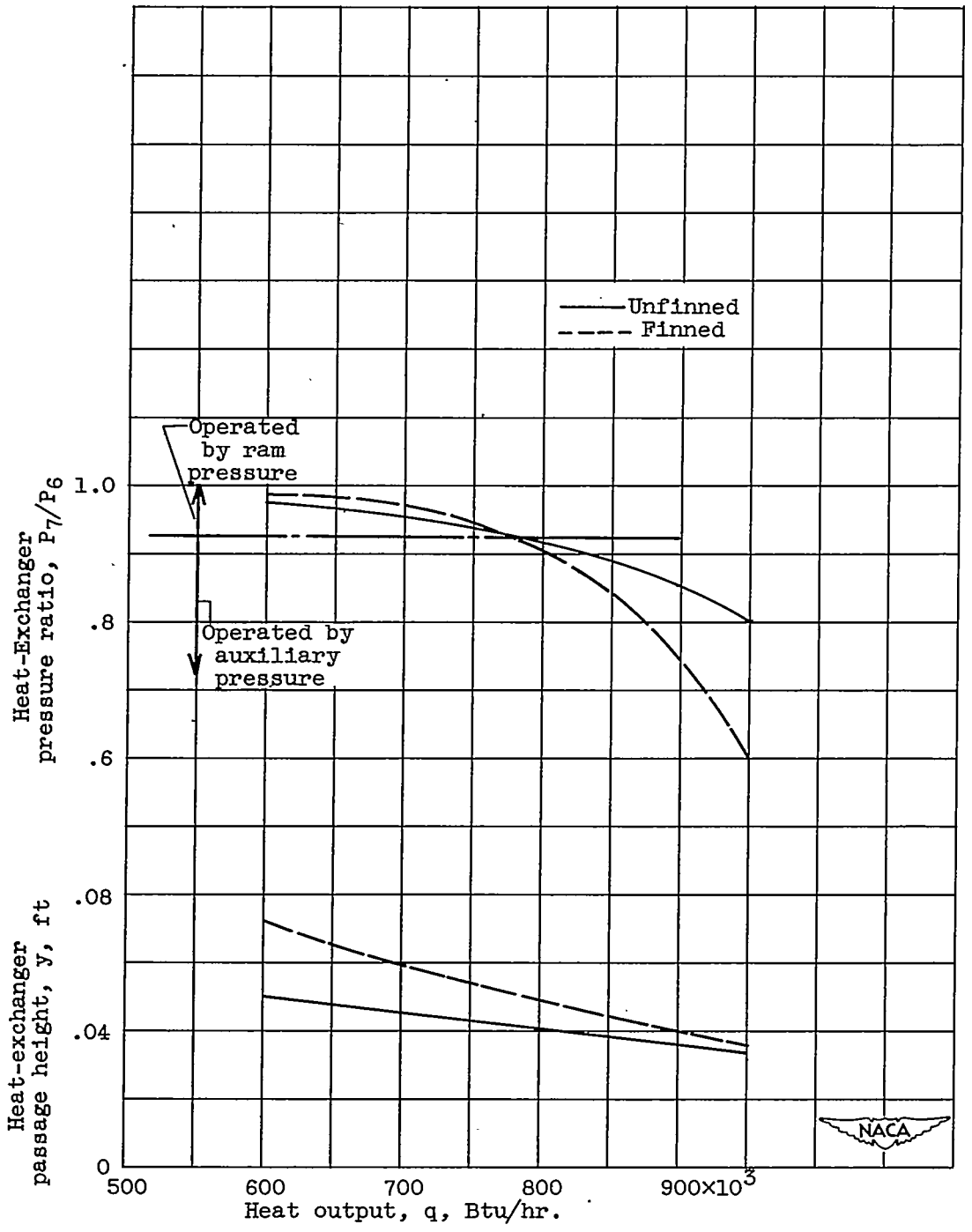

Figure 12. - Comparison of performance of finned and unfinned heat exchangers at flight Mach number of 0.5 and altitude of 15,000 feet. Outlet air temperature, 800° F; tail-pipe diameter, 2.17 feet; rated engine gas flow, 147 pounds per second; heat-exchanger length, 6 feet.

NACA-Langley - 9-4-51 - 1000